Copy No. _____

Guide for Mechanistic-Empirical Design
OF NEW AND REHABILITATED PAVEMENT STRUCTURES

FINAL DOCUMENT

APPENDIX NN:
CALIBRATION OF REHABILITATION OF EXISTING PAVEMENTS WITH PCC

NCHRP

Prepared for
National Cooperative Highway Research Program
Transportation Research Board
National Research Council

Submitted by
ARA, Inc., ERES Division
505 West University Avenue
Champaign, Illinois 61820

August 2003

Acknowledgment of Sponsorship

This work was sponsored by the American Association of State Highway and Transportation Officials (AASHTO) in cooperation with the Federal Highway Administration and was conducted in the National Cooperative Highway Research Program which is administered by the Transportation Research Board of the National Research Council.

Acknowledgements

The research team for NCHRP Project 1-37A: Development of the 2002 Guide for the Design of New and Rehabilitated Pavement Structures consisted of Applied Research Associates, Inc., ERES Consultants Division (ARA-ERES) as the prime contractor with Arizona State University (ASU) as the primary subcontractor.

Research into the subject area covered in this Appendix was conducted at ARA-ERES. The author of this Appendix is Mr. Leslie Titus-Glover. Dr. Darter provided technical and managerial coordination of the Rehabilitation with PCC design group, monitored progress, set schedules and deadlines, and provided periodic technical review of research results as they became available. Mr. Jag Mallela provided assistance with technical and managerial coordination.

Foreword

This appendix presents a detailed summary of the verification and validation (and when required re-calibration) of distress prediction models originally developed for new PCC (jointed plain concrete pavement [JPCP] and continuously reinforced concrete pavement [CRCP]) design to determine their suitability for rehabilitation of existing pavements (flexible, composite, and rigid) with PCC design. PCC rehabilitation of existing pavement design alternatives considered in the Design Guide and described in this appendix are as follows:

- JPCP restoration.
- Unbonded JPCP or CRCP over existing PCC.
- Bonded PCC over existing JPCP or CRCP.
- JPCP or CRCP overlay over existing flexible pavement.

The information contained in this appendix serves as a supporting reference to PART 3, Chapter 7 of the Design Guide.

APPENDIX NN

CALIBRATION OF REHABILITATION OF EXISTING PAVEMENTS WITH PCC

1.0 Introduction

The objective of NCHRP Project 1-37A was to develop a guide for the design of new and rehabilitated pavement structures based on mechanistic-empirical (M-E) principles. An M-E based Design Guide will provide the highway community with a state-of-the-practice tool for the design of pavement structures representing a major paradigm shift in current empirical design procedures. The PCC rehabilitation design procedure outlined in this Guide is very similar to that of new PCC pavement design described in Part 3—DESIGN ANALYSIS, Chapter 4 of this Guide. Key aspects of design such as the pavements material, traffic, and climate characterization are essentially the same. Because of the mechanistic based principles used, the models and algorithms used to compute pavement responses such as stress, strain, deflections, damage, and distress are applicable to both new PCC design and PCC rehabilitation design.

Mechanistic analysis make it possible to extend the use of distress prediction models developed for new PCC design to PCC rehabilitation design. However, the PCC design models used in PCC rehabilitation design must be verified and validated to ensure their suitability for predicting distress within the inference space of PCC rehabilitated pavements.

This appendix presents a detailed summary of the verification and validation (and when required re-calibration) of distress prediction models developed for new PCC (jointed plain concrete pavement [JPCP] and continuously reinforced concrete pavement [CRCP]) design to determine if they are suitable for use for PCC rehabilitation design of existing pavements (flexible, composite, and rigid). PCC rehabilitation of existing pavement design alternatives considered in the 2002 design procedure were:

- JPCP restoration (i.e., concrete pavement repair [CPR] including diamond grinding) for existing JPCP only.
- Unbonded JPCP over existing PCC (JPCP, jointed reinforced concrete pavement [JRCP], and CRCP).
- Bonded PCC over existing JPCP or CRCP.
- JPCP or CRCP overlay over existing flexible pavement.
- Reconstruction with JPCP or CRCP.

Verification, validation, and recalibration was done by applying both analytical and statistical techniques. Where the results of verification and calibration showed that the new PCC design distress prediction models were inadequate the PCC distress models were recalibrated to determine the best set of model coefficients that could be used to predicted distress with accuracy while minimizing error. The distress models presented in this appendix are for PCC rehabilitation design only. A description of HMAC rehabilitation design distress models are described in Appendix MM. Also, a comprehensive description of the M-E based design models

for new PCC pavement design have been presented and discussed in several chapters of the 2002 Design Guide and in several appendices. These chapters and appendices describe in-depth how the models were developed, how the models were applied, and how input parameters such as pavement material and design properties, traffic, and climate were characterized.

2.0 Overview of Model Verification and Validation

The goal of verification and validation is to determine whether distress models for new PCC design when applied to PCC rehabilitation design would predict distress accurately with minimal bias and reasonable error. When properly done, verifying and validating a model should lead to improving the model's credibility with users and improve upon the reliability of the entire PCC rehabilitation design procedure. Verification and validation for this study is defined as follows:

- Verification is comparing the conceptual model and algorithms with actual field observed trends and estimates or trends and estimates determined from mechanistic analysis (1).
- Validation is ensuring that a model within its domain of applicability possesses a satisfactory range of accuracy consistent with the intended application of the model (2).

3.0 Framework for Model Verification and Validation

Model verification and validation consisted of the following steps:

1. Conduct a preliminary verification of all algorithms and models.
2. Comparison of model distress predictions to observed distress (measured from in-service pavements).
3. Perform a comprehensive sensitivity analysis.

<u>Preliminary Verification of All Algorithms and Models</u>

Preliminary verification of algorithms and models consisted of determining whether all the algorithms and pavement response models used in estimating stress, deflection, load transfer, crack width, and distress for new PCC design models work reasonably well within the inference space for PCC rehabilitation design. As an example, can the algorithm developed to estimate stress and deflections in a new JPCP over an asphalt treated base be used to determine the same stresses and deflections for a JPCP overlay over an existing HMAC? Note that AC-treated materials and HMAC could have very different gradations, resilient modulus, binder type and content, voids, and so on.

Preliminary verification of algorithms and models was done as follows:

1. Identify different PCC rehabilitation design scenarios that represent selected PCC rehabilitation alternatives (e.g., JPCP restoration, unbonded JPCP over existing PCC, bonded PCC over existing CRCP, and so on).
2. Develop input parameters for each scenario (i.e., each PCC rehabilitation alternative).

3. Use the inputs for each scenario to estimate key pavement responses such as stress, deflection, joint load transfer efficiency (LTE), damage, and so on and predict distress (transverse joint faulting and transverse cracking for JPCP and punchouts for CRCP).
4. Examine all outputs for reasonableness (values of estimates, trends, etc).

It can be concluded that the new PCC design models are suitable for PCC rehabilitation design if the outcome of steps 1 through 4 is determined to be reasonable. Where the outcome was determined not to be reasonable it was necessary to modify the new PCC design algorithms and distress models to improve upon their applicability to PCC rehabilitation design or modify calibration constants, or both.

Comparison of Model Distress Predictions to Observed Distress

Comparison of model predicted distress and actual field measurements of distress is the next important step in model verification and validation as this shows the ability of the new PCC design models to accurately predict distress for PCC rehabilitation design. Comparisons were made by applying the following steps:

1. Assemble a database of in-service PCC rehabilitated test pavements. The database must contain the test pavements design, material, construction, climate, traffic, and measured pavement distress and IRI.
2. For each test pavement, run the relevant new PCC design distress models using the input data assembled in step 1.
3. Compare the new PCC design models predicted distress to measured distress (from the in-service pavement test sections) and evaluate the predictive capacity and accuracy of the distress models.

The predictive capacity and accuracy of the distress models were evaluated using statistical analysis as follows:

1. Determine the correlation between predicted and measured distress (R^2).
2. Determine the residual error between predicted and measured distress (mean square error, [MSE]).
3. Use paired t-tests to determine whether there is a significant difference on average between measured and predicted distress for the in-service pavements analyzed.

The statistical analysis was conducted using data obtained from in-service rehabilitated pavements located in North America. Note that comparisons of model predicted distress and measured distress was done only after the new PCC design algorithms and models had been determined to be reasonable based on the preliminary analysis described in the preceding sections.

Sensitivity Analysis (Test Model over Range of Input Parameters)

The final step in model verification and validation was sensitivity analysis. Sensitivity analysis is the determination of how variations in input parameters quantitatively affect predicted distress and IRI. The goals of a sensitivity analysis are as follows:

- If the PCC design distress prediction models can simulate observed trends in the development and progression of distress.
- What factors contribute to variability in the predicted distress (and may require additional research to strengthen the knowledge base).
- What model parameters (or parts of the model itself) are significant or insignificant?
- If and which (group of) input parameters interact with each other.

To run an effective sensitivity analysis it must be ensured that the entire range of each significant input parameter is examined individually along with their interaction with other input variables (e.g., interaction between PCC flexural strength and elastic modulus). The general approach adopted in this study was to repeatedly run each new PCC design distress prediction model for different combinations of input parameters within the expected inference space for PCC rehabilitated pavements (e.g., unbonded JPCP overlay thickness ranges from 6 to 15 in) and then evaluating the predicted distress and IRI for reasonableness. The steps used in sensitivity analysis are as follows:

1. Determine key input parameters.
2. Assign typical ranges for the key input parameters selected.
3. Create virtual PCC rehabilitated pavement test sections based on the parameters selected and their ranges.
4. Run the new PCC design distress prediction models to predict distress and IRI for each virtual PCC rehabilitated test section.
5. Assess the reasonableness of the predicted distress and the relative importance and sensitivity of each input parameter.

Reasonableness was assessed by determining the percentage of the total amount of variation in predicted distress that each input parameter accounts for (when all others input parameters are kept at some constant level) and observing the trends in predicted distress with increasing age or traffic applications.

4.0 Preliminary Verification of All Algorithms and Models

Four scenarios representing different rehabilitation alternatives were used to preliminarily determine the reasonableness of all algorithms and models used for new PCC design and adopted for PCC rehabilitation design. The algorithms and distress models evaluated were as follows:

- Algorithms.
    - JPCP joint load transfer efficiency (LTE).
    - JPCP differential energy (DE).
    - JPCP fatigue damage (top-down and bottom up).

    - CRCP crack load transfer efficiency (LTE).
    - CRCP crack width.
- Models
    - JPCP transverse joint faulting.
    - JPCP transverse cracking.
    - CRCP punchouts.

The four scenarios were as follows:

1. Restored JPCP (existing JPCP subjected to concrete pavement repairs (CPR) including diamond grinding).
2. Unbonded JPCP over existing PCC.
3. Bonded PCC over existing CRCP.
4. JPCP overlay over existing flexible pavement.

The results are described in the following sections.

Scenario 1—Restored JPCP

Inputs

Data from the LTPP test section 01_0605 was used in creating scenario 1—existing JPCP subjected to CPR including full-depth patching, diamond grinding, full-depth joint repair, and shoulder replacement with HMAC. A summary of the input parameters are presented in table 1. A detailed description of all inputs is presented in Appendix LL. The inputs were used to estimate key pavement responses and distress using the new PCC design models. Estimates of the key pavement responses and predicted mean transverse joint faulting and transverse cracking are presented in figures 1 through 4.

Summary of Results

The plots presented in figures 1 through 5 shows reasonable estimates of the key pavement responses and distress. The trends observed are summarized as follows:

- Decreasing LTE with increasing age and traffic applications.
- Variations in LTE with seasons.
- Increasing faulting with increasing age and traffic applications (S-shaped curve).
- Increasing fatigue damage (top-down and bottom up) with increasing age and traffic applications.
- Increasing transverse cracking with increasing age and traffic applications.

In general, the observed trends were in agreement with those observed through field measurements and mechanistic analysis. Also, the effects of climate on pavement responses such as LTE was as expected.

Table 1. Summary of input parameters for scenario 1—restored JPCP.

• Design Life	10 years
• Pavement construction date:	May, 1966
• Pavement restoration date:	June, 1998
• Two-way average annual daily truck traffic:	1700
• Cumulative number of heavy trucks (after 10 years):	3,541,070
• Joint spacing:	20 ft
• Dowel diameter:	0 in
• Edge Support	None
• Number of layers:	3
• Layer 1—JPCP	
o Thickness:	10 in
o Compressive strength:	5900 psi
• Layer 2—Unbound material AASHTO class A-1-a	
o Thickness:	6 in
o Resilient modulus:	40000 psi
• Layer 3— Unbound material AASHTO class A-6	
o Thickness:	Semi-infinite
o Resilient modulus:	17000 psi
• Existing pavement condition	
o Percent slabs with transverse cracks (plus replaced slabs):	8
o Percent of slabs with repairs after restoration:	8

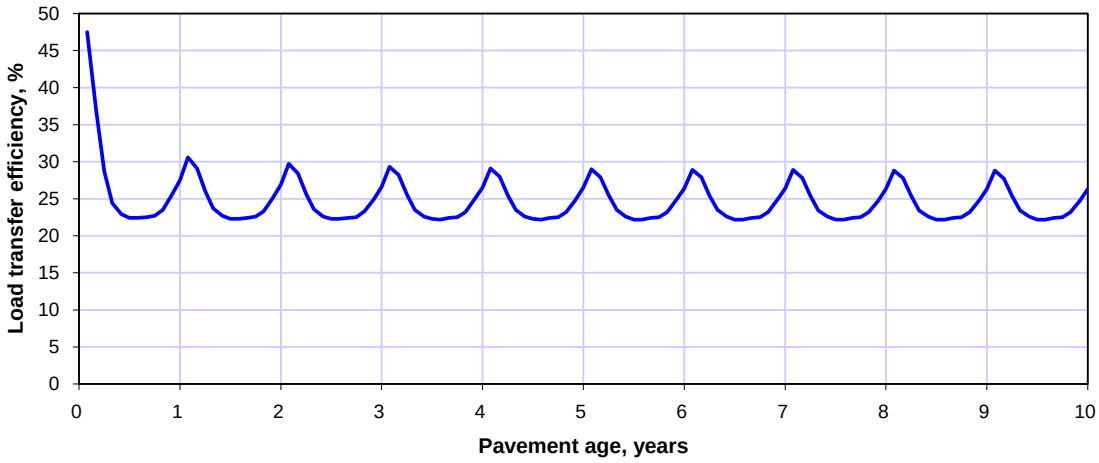

Figure 1. Plot of pavement age versus LTE for restored JPCP.

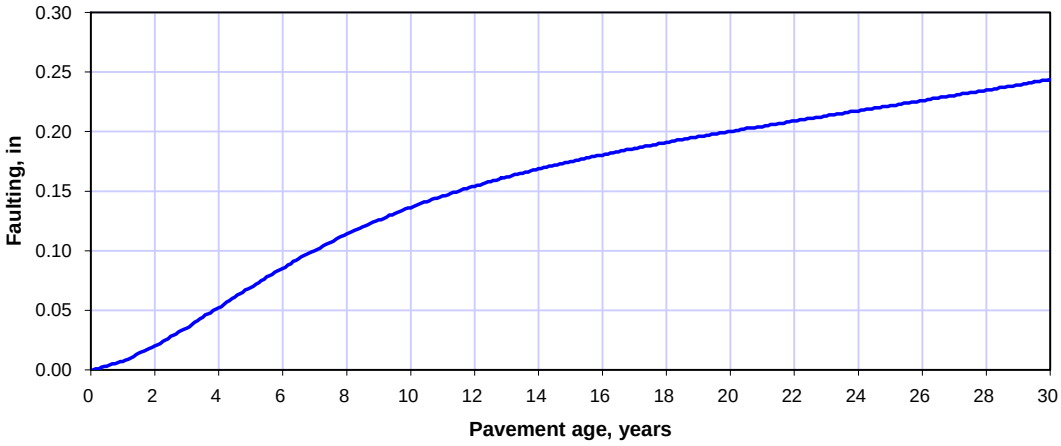

Figure 2. Plot of pavement age versus faulting for restored JPCP.

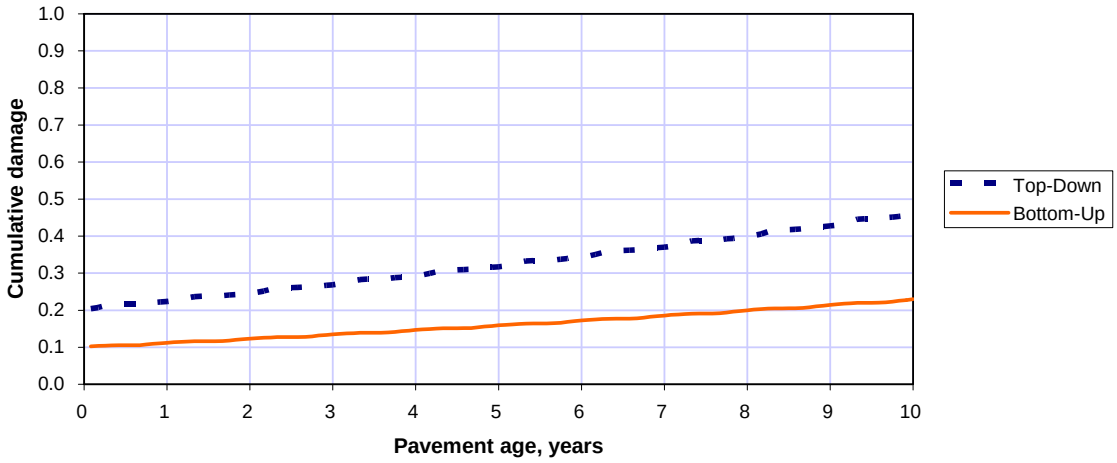

Figure 3. Plot of pavement age versus fatigue damage for restored JPCP.

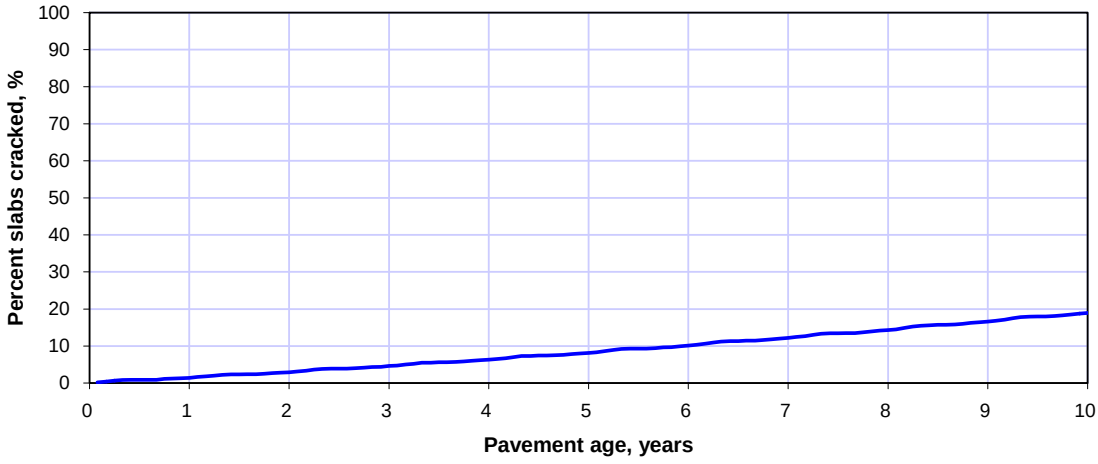

Figure 4. Plot of cracking (existing and additional after restoration minus repairs) versus pavement age for restored JPCP.

Scenario 2—Unbonded JPCP over Existing Rubblized PCC (with HMAC Separator Layer)

Inputs

Data from the LTPP test section 20_9037 was used in creating scenario 2—unbonded JPCP overlay over an existing PCC (after CPR). A summary of the input parameters are presented in table 2. A detailed description of all inputs is presented in Appendix LL. Estimates of key pavement responses and predicted mean transverse joint faulting and transverse cracking are presented in figures 5 through 8.

Summary of Results

The plots presented in figures 5 through 8 shows reasonable estimates of the key pavement responses and distress. The trends observed are summarized as follows:

- Decreasing LTE with increasing age and traffic applications.
- Variations in LTE with seasons.
- Increasing faulting with increasing age and traffic applications.
- Increasing fatigue damage (top-down and bottom up) with increasing age and traffic.
- Increasing transverse cracking with increasing age and traffic applications.

These trends are in agreement with those observed through field measurements and mechanistic analysis. Also, the effects of climate on pavement responses such as LTE was as expected. It appears that the algorithms and models developed for new pavement design can be extended to unbonded JPCP overlays over existing PCC reasonably well. The preliminary estimates and trends show that the new PCC design models have the capability of modeling pavement responses and predicting distress for unbonded JPCP overlays. Further analysis (presented in sections 6 and 7 of this appendix) would be required to determine the suitability of the new PCC design models for PCC rehabilitation design.

Scenario 3—Bonded PCC over Existing CRCP

Inputs

Data from the LTPP test section 19_0702 was used in creating scenario 3—bonded PCC over existing CRCP. A summary of the input parameters are presented in table 3. A detailed description of all inputs is presented in Appendix LL. Estimates of key mechanistic parameters and predicted punchouts over time obtained from the new PCC design models are presented in figures 9 through 11.

Table 2. Summary of input parameters for scenario 2—unbonded JPCP over existing PCC pavement.

• Design Life	30 years
• Pavement construction month:	June, 1968
• Traffic open month:	August, 1968
• Two-way average annual daily truck traffic:	4,625
• Cumulative number of heavy trucks (after 10 years):	27,911,700
• Joint spacing:	15.5 ft
• Dowel diameter:	0 in
• Edge Support	None
• Number of layers:	5
• Layer 1—JPCP	
o Thickness:	7.5 in
o 28-day compressive strength:	6384 psi
• Layer 2—HMAC (Separator Layer)	
o Thickness:	1.0 in
o AC dynamic modulus:	228,000 psi
• Layer 3—PCC (rubblized)	
o Thickness:	7.7 in
o Elastic modulus:	201,600 psi
• Layer 4—Cement stabilized material	
o Thickness:	3.4 in
o Modulus:	300,000 psi
• Layer 5— Unbound material AASHTO class A-3	
o Thickness:	Semi-infinite
o Modulus:	29000 psi

Figure 5. Plot of pavement age versus LTE for unbonded JPCP overlay over existing PCC.

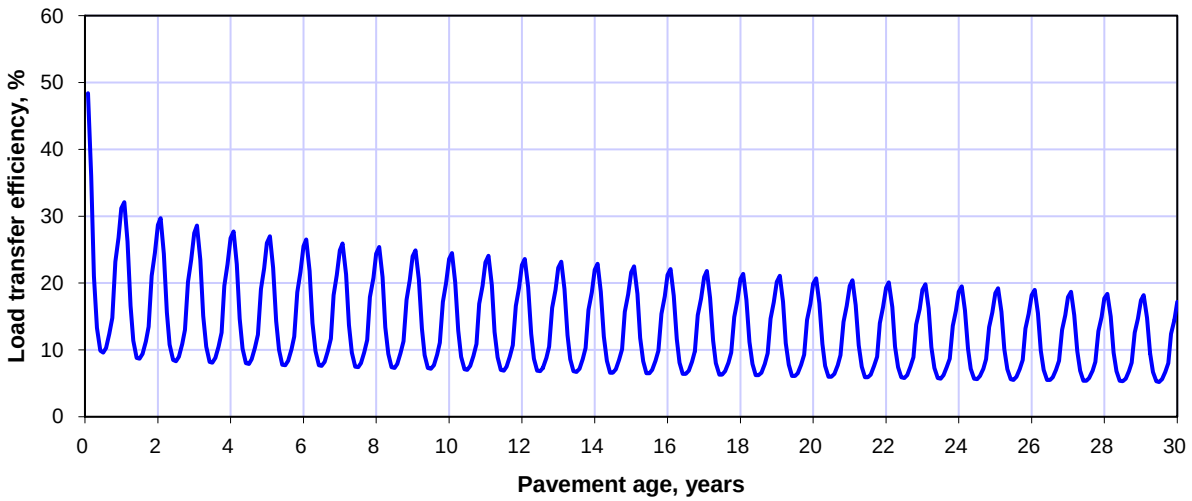

Figure 6. Plot of pavement age versus faulting for unbonded JPCP overlay over existing PCC.

Figure 7. Plot of pavement age versus fatigue damage for unbonded JPCP overlay over existing PCC.

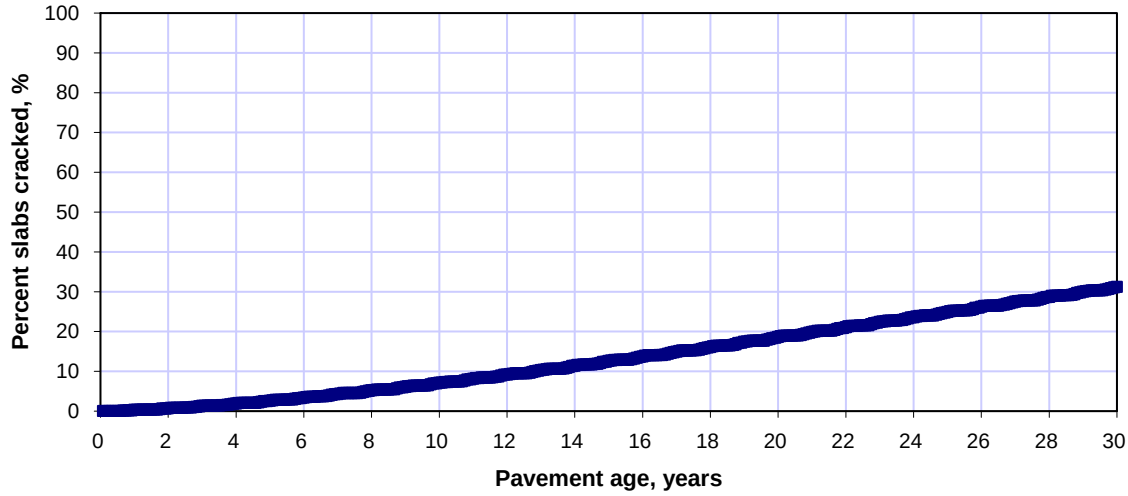

Figure 8. Plot of cracking versus pavement age for unbonded JPCP overlay over existing PCC.

Table 3. Summary of input parameters for scenario 3—bonded PCC over existing CRCP.

• Design Life	10 years
• Pavement construction month:	September, 1992
• Traffic open month:	October, 1992
• Two-way average annual daily truck traffic:	1600
• Cumulative number of heavy trucks (after 10 years):	2870280
• Percent steel (%):	0.63
• Bar diameter (in):	0.625
• Steel depth (in):	3.4
• Base type:	Granular
• Erodibility index:	Erosion Resistance (3)
• Base/slab friction coefficient:	1.5
• Number of layers:	4
• Layer 1—PCC	
o Thickness:	4.5 in
o 28-day compressive strength:	4813 psi
• Layer 2—CRCP	
o Thickness:	6.0 in
o 28-day compressive strength:	5451 psi
• Layer 4—Unbound material AASHTO class A-1-a	
o Thickness:	7.8 in
o Modulus:	38000 psi
• Layer 4—Unbound material AASHTO class A-6	
o Thickness:	24 in
o Modulus:	17000 psi
• Layer 5— Unbound material AASHTO class A-6	
o Thickness:	Semi-infinite
o Modulus:	17000 psi

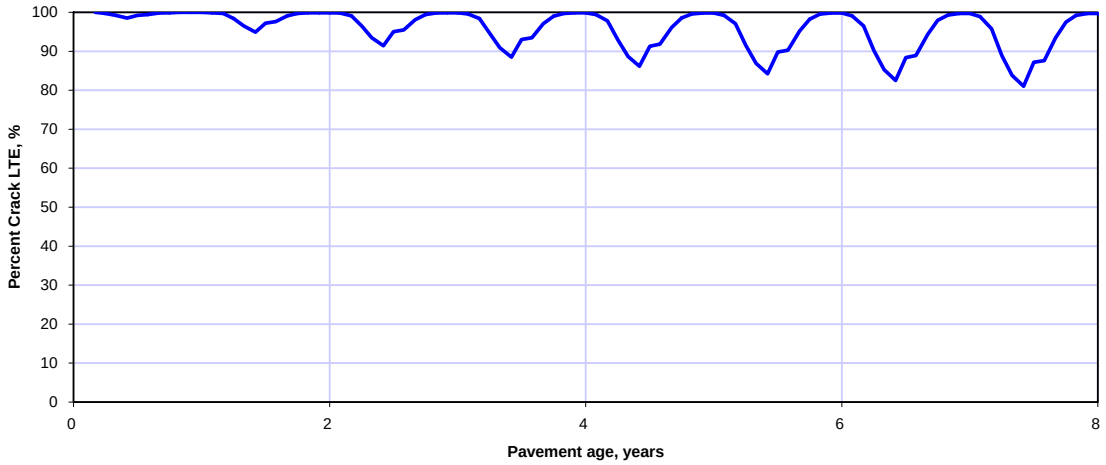

Figure 9. Plot of pavement age versus LTE for bonded PCC overlay over existing CRCP.

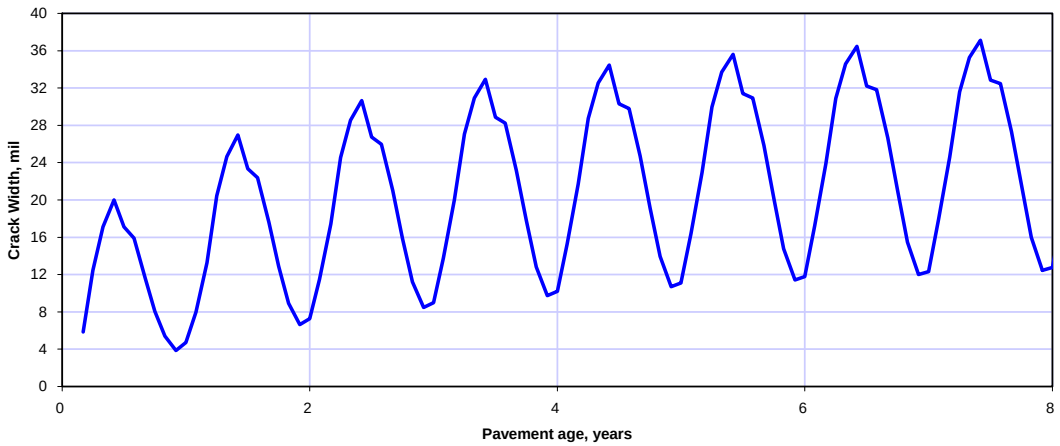

Figure 10. Plot of pavement age versus crack width for bonded PCC overlay over existing CRCP.

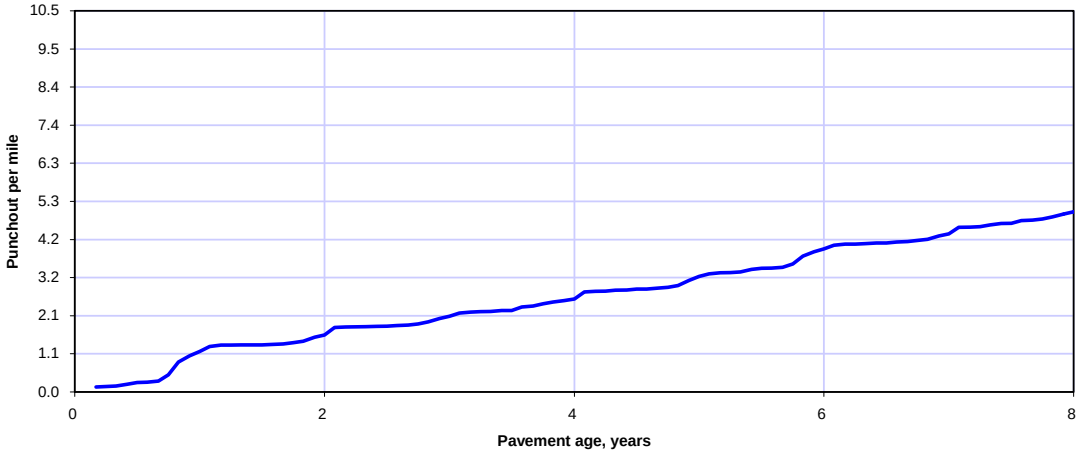

Figure 11. Plot of pavement age versus punchouts bonded PCC overlay over existing CRCP.

Summary of Results

The plots presented in figures 9 through 11 shows reasonable estimates of the key CRCP responses and distress. The trends observed are summarized as follows:

- Increasing crack width with increasing age and traffic applications.
- Decreasing crack LTE with increasing age and traffic applications.
- Variations of crack width with seasons.
- Increasing punchouts with increasing age and traffic applications.

The crack LTE also varied appropriately with seasons. These trends are in agreement with those observed through field measurements and mechanistic analysis.

It appears that the algorithms and models developed for new CRCP design can be extended to bonded PCC overlays over existing CRCP reasonably well. The preliminary estimates and trends

show that the new CRCP design models have the capability of modeling pavement performance and predicting distress for bonded PCC overlays over existing CRCP. Further analysis (presented in sections 6 and 7 of this appendix) is required to determine the suitability of the new CRCP design models for PCC rehabilitation design.

Scenario 4—JPCP Overlay over Existing Flexible Pavement

Inputs

Data used in the design of a JPCP overlay over existing flexible pavement project in Kansas was used in creating scenario 4—JPCP overlay over existing flexible pavement. A summary of the input parameters are presented in table 4. A detailed description of all inputs is presented in Appendix LL. Estimates of key pavement responses and predicted transverse joint faulting and transverse cracking over time obtained from the new PCC design models are presented in figures 12 through 15.

Summary of Results

The plots presented in figures 15 through 19 shows reasonable estimates of the key JPCP responses and distress. The trends observed are summarized as follows:

- Decreasing joint LTE with increasing age and traffic applications.
- Variations in joint LTE with seasons.
- Increasing faulting with increasing age and traffic applications.
- Increasing fatigue damage (top-down and bottom up) with increasing age and traffic applications.
- Increasing transverse cracking with increasing age and traffic applications.

These trends are in general agreement with those observed through field measurements and mechanistic analysis. Also, the effects of climate on pavement responses such as LTE was as expected.

Table 4. Summary of input parameters for scenario 4—JPCP overlay over existing flexible pavement.

• Design Life	30 years
• Pavement construction month:	July, 1996
• Traffic open month:	August, 1996
• Two-way average annual daily truck traffic:	1250
• Cumulative number of heavy trucks (after 30 years):	8628600
• Overlay JPCP joint spacing:	15 ft
• Dowel diameter:	1 in
• Edge Support	Widened lane (slab width = 13 ft)
• Number of layers:	5
• Layer 1—JPCP	
o Thickness:	7.0 in
o 28-day flexural strength:	650 psi
• Layer 2—HMAC	
o Thickness:	12.0 in
o Dynamic modulus:	2000000 psi (based on level 3 binder, gradation and mixture properties)
• Layer 3—Crushed gravel	
o Thickness:	10.0 in
o Elastic modulus:	23000 psi
• Layer 4—Crushed gravel	
o Thickness:	10.0 in
o Modulus:	23000 psi
• Layer 5— Unbound material AASHTO class A-6	
o Thickness:	Semi-infinite
o Modulus:	8400 psi

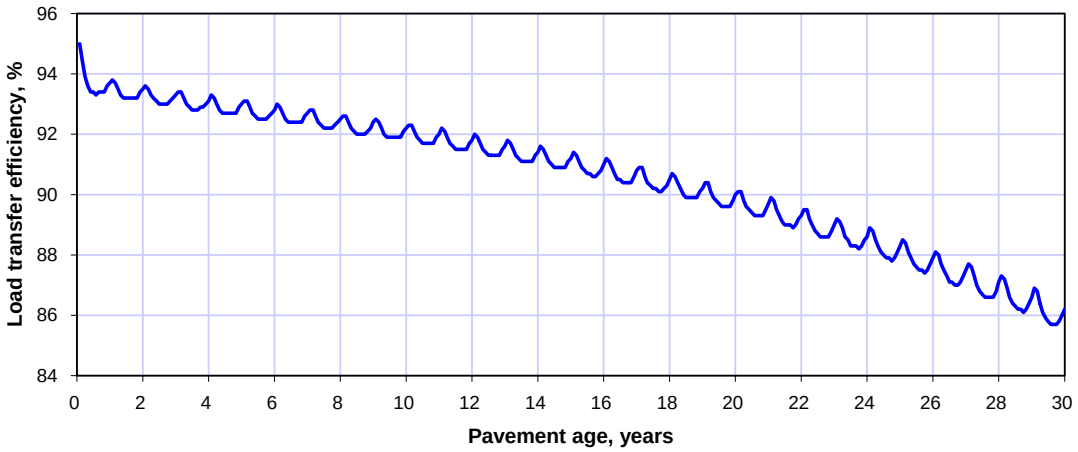

Figure 12. Plot of pavement age versus LTE for JPCP overlay over existing flexible pavement.

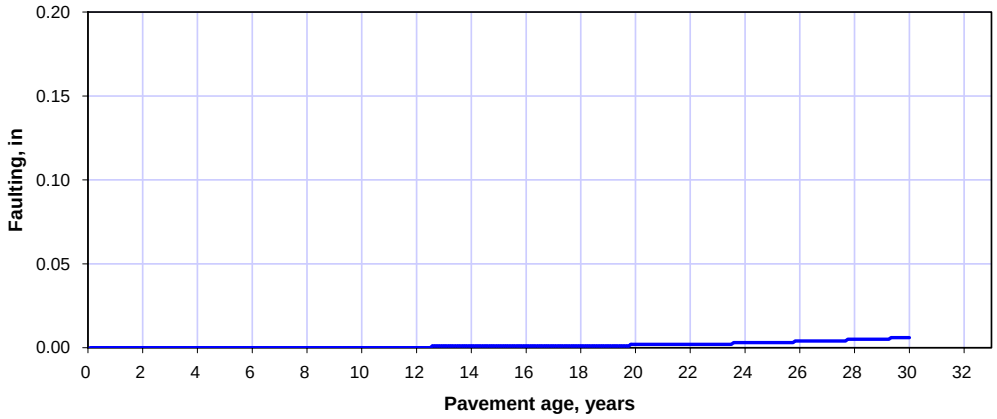

Figure 13 Plot of pavement age versus faulting for JPCP overlay over existing flexible pavement.

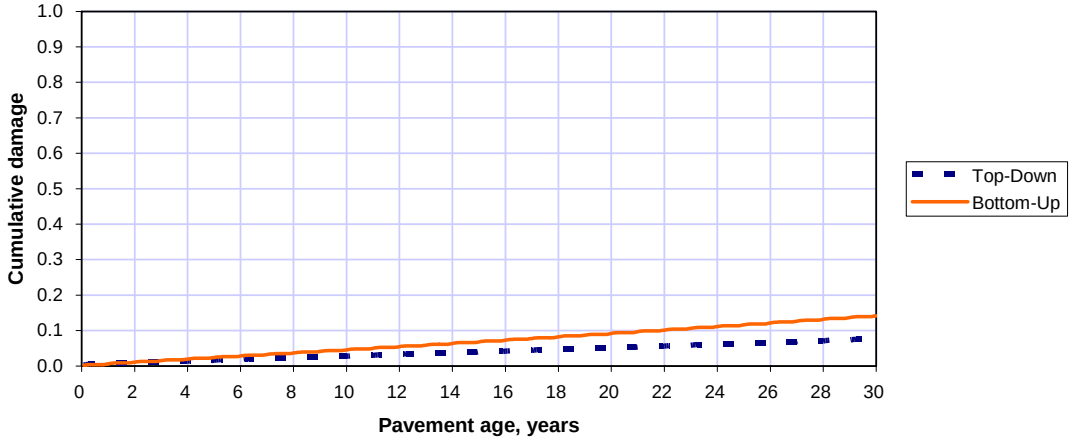

Figure 14. Plot of pavement age versus fatigue damage for JPCP overlay over existing flexible pavement.

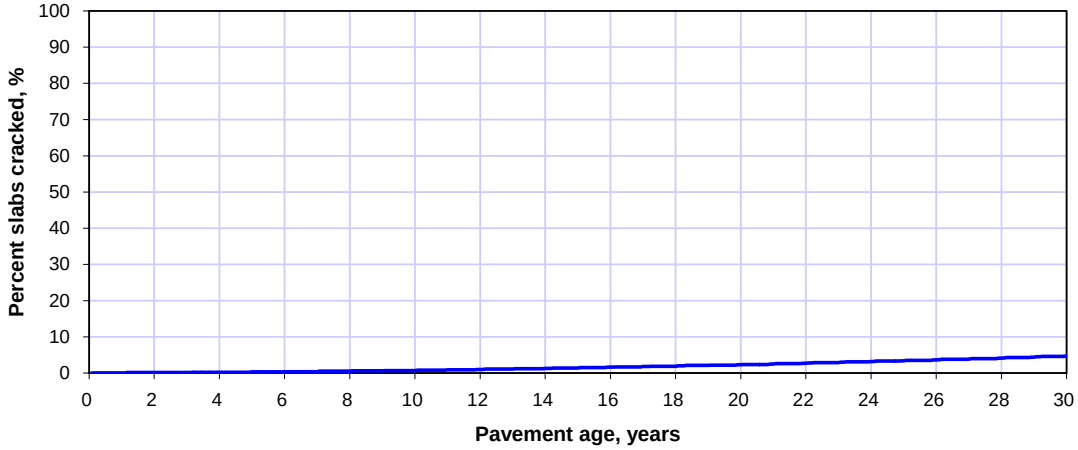

Figure 15. Plot of cracking versus pavement age for JPCP overlay over existing flexible pavement.

It appears that the algorithms and models developed for new JPCP design can be extended to JPCP overlays over existing flexible pavement reasonably well. The preliminary estimates and trends show that the new JPCP design models have the capability of modeling pavement responses and predicting distress for JPCP overlays over existing flexible pavements. Further analysis (presented in sections 6 and 7 of this appendix) is required to determine the suitability of the new PCC models for PCC rehabilitation design.

5.0 Model Description

The model types considered in rehabilitation with PCC were:

- Faulting.
- Transverse cracking.
- Punchouts.

Detailed descriptions of these are presented for new PCC design in appendices JJ, KK, and LL for transverse joint faulting, transverse cracking, and CRCP punchouts, respectively. The transverse joint faulting and transverse cracking models were modified to make them more suitable for JPCP restoration (including diamond grinding) design. Descriptions of the modified models are presented in the following sections.

Transverse Joint Faulting

Transverse joint faulting is the differential elevation across the joint measured approximately 1 ft from the slab edge (longitudinal lane to shoulder joint for a conventional 12-ft lane width), or from the lane paint stripe for a widened slab. Since joint faulting varies significantly from joint to joint, the mean faulting of all transverse joints in a given section is the parameter predicted by the model used in this Guide for performance evaluation. Faulting is an important deterioration mechanism of JPCP because of its impact on ride quality. Joint faulting also has a major impact on the life cycle costs of rehabilitated pavements, both in terms of increased costs due to early failure of the rehabilitation strategy and on vehicle operating costs as faulting becomes severe. Transverse joint faulting is the result of a combination of moving heavy axle loads, poor joint load transfer, free moisture beneath the PCC slab and or base, and base/subbase erosion. Equations 1 through 4 are used to predict transverse joint faulting for restored JPCP and JPCP overlays:

$$Fault_m = \sum_{i=1}^{m} \Delta Fault_i \tag{1}$$

$$\Delta Fault_i = C_{34} * (FAULTMAX_{i-1} - Fault_{i-1})^2 * DE_i \tag{2}$$

$$FAULTMAX_i = FAULTMAX_0 + C_7 * \sum_{j=1}^{m} DE_j * Log(1 + C_5 * 5.0^{EROD})^{C_6} \tag{3}$$

$$FAULTMAX_0 = C_{12} * \delta_{curling} * \left[Log(1 + C_5 * 5.0^{EROD}) * Log(\frac{P_{200} * WetDays}{p_s}) \right]^{C_6} \tag{4}$$

where

$Fault_m$	=	mean joint faulting at the end of month m, in (at 50 percent reliability)
$\Delta Fault_i$	=	incremental change (monthly) in mean transverse joint faulting during $month_i$, in
$FAULTMAX_i$	=	maximum mean transverse joint faulting for month , in
$FAULTMAX_0$	=	initial maximum mean transverse joint faulting, in
EROD	=	base (layer beneath the PCC slab) erodibility factor
DE_i	=	differential deformation energy accumulated during month i
$\delta curling$	=	maximum mean monthly slab corner upward deflection PCC due to temperature curling and moisture warping
p_S	=	overburden on subgrade, psi
P_{200}	=	percent subgrade material passing #200 sieve
WetDays	=	average annual number of wet days
C_{12}	=	$C_1 + C_2*FR^{0.25}$
C_{34}	=	$C_3 + C_4*FR^{0.25}$
FR	=	base freezing index defined as percentage of time the top base temperature is below freezing (32^oF) temperature.
C_1 through C_7	=	calibration constants

Equations 1 through 4 were developed and calibrated for new pavements as described in Part 3—DESIGN ANALYSIS, Chapter 4 and Appendix JJ. Note that the model coefficients were modified to make them suitable for restored JPCP design.

Transverse Cracking

Transverse cracking is an important deterioration mechanism of restored JPCP and JPCP overlays because it represents the principal structural deterioration mode of JPCP. Cracking also affects ride quality when the cracks deteriorate and fault. For JPCP transverse cracking, two modes of failure are considered:

- Bottom-up cracking.
- Top-down cracking.

Under typical service conditions, the potential for either mode of cracking is present in all slabs. Any given slab may crack either from the bottom-up or the top-down, but not both. Therefore, the predicted bottom-up and top-down cracking are not particularly meaningful by themselves, and combined cracking must be determined, excluding the possibility of both modes of cracking occurring on the same slab. JPCP transverse cracking is predicted using equation 5 below:

$$TCRACK = \left(CRK_{Bottom-up} + CRK_{Top-down} - CRK_{Bottom-up} \cdot CRK_{Top-down}\right)*100 - CRK_{REPAIRED} \quad (5)$$

where

TCRACK	=	total cracking (percent slabs)

$CRK_{Bottop\text{-}up}$ = predicted amount of bottom-up cracking (fraction).
$CRK_{Top\text{-}down}$ = predicted amount of top-down cracking (fraction).
CRK_{Repair} = percent of existing transverse cracks repaired (for restored JPCP only; otherwise, it is assumed to be zero).

The model combines bottom-up and top-down cracking to obtain total cracking. The procedure for estimating fatigue damage and transverse cracking due to the bottom-up and top-down cracking mechanisms is presented in Appendix KK and Part 3—DESIGN ANALYSIS, Chapter 4. The expected amount of cracking from each mode is then calculated separately.

The general expression for fatigue damage accumulations (for both bottom-up and top-down mechanisms) is as follows:

$$FD = IDAM + \sum \frac{n_{i,j,k,l,m,p}}{N_{i,j,k,l,m,p}} \quad (6)$$

where,
$n_{i,j,k,...}$ = applied number of load applications at condition *i,j,k,…*
$N_{i,j,k,...}$ = allowable number of load applications at condition *i,j,k,…*
IDAM = estimate of past bottom-up or top-down fatigue damage (see Note 1)
i = age (accounts for change in PCC modulus of rupture, layer bond condition, deterioration of shoulder LTE)
j = season (accounts for change in base and effective modulus of subgrade reaction)
k = axle type (singles, tandems, and tridems)
l = load level (incremental load for each axle type)
m = temperature difference (probability distribution [2 °F increments ranging from 10 °F to 40 °F] applied to total traffic within the time interval); the "effective temperature difference" due to construction curling and moisture warping is subtracted from the temperature gradient for stress computation
p = traffic path (mean position and standard deviation used to obtain probability function of load position; Gauss integration scheme discussed in Part 3—DESIGN ANALYSIS, Chapter 4 is used for computation efficiency and accuracy)

For restored JPCP, the initial bottom-up and top-down fatigue damage is required when computing future bottom-up and top-down fatigue damage. For bonded PCC over JPCP, only the initial bottom-up fatigue damage is required since initial top-down fatigue damage in the overlay PCC is assumed to be zero. Initial bottom-up and top-down fatigue damage is assumed to be zero for all other overlay types. A description of the procedure for estimating initial fatigue damage is presented later in this appendix.

The applied number of load applications ($n_{i,j,k,l,m,n}$) is the actual number of axle combination *k* of load level *l* that passed through traffic path *n* under each condition (age, season, and temperature difference). The allowable number of load applications is the number of load cycles at which fatigue failure is expected (corresponding to 50 percent slab cracking) and is a function of the applied stress and PCC strength. The allowable number of load applications is determined using the following fatigue model**:**

$$\log\left(N_{i,j,k,l,m,n}\right) = C_1 \cdot \left(\frac{M_R}{\sigma}\right)^{C_2}_{i,j,k,l,m,p} \quad (7)$$

where

N	=	allowable number of load applications (cracking)
MR	=	PCC modulus of rupture, psi
σ	=	applied stress calculated using axle combination k of load level l that passed through traffic path n under a given set of conditions (age, season, and temperature difference)
C_1, C_2	=	calibration constants

Note that the location of the critical stresses for bottom-up and top-down cracking is different. The differences in the joint spacing calls for use of different neural networks for computing top-down stresses (the appropriate NN to use is described in Part 3—DESIGN ANALYSIS, Chapter 4). Also, unlike bottom-up cracking, the location of critical damage is not predefined for top-down cracking. The critical damage location depends on axle load distribution, temperature gradients, permanent curl/warp, joint spacing, and axle spacing, and it could be any point along the lane-shoulder joint between about 36 in and 0 in from the middle of the slab (mid-point between two transverse joints along the lane-shoulder joint). A procedure used to locate the exact location of the critical damage is presented in Part 3—DESIGN ANALYSIS, Chapter 4.

The fatigue damages calculated for bottom-up and top-down cracking are mechanistic parameters that represent the occurrence and coalescing of micro-cracks to form larger cracks at the bottom and top of the PCC slabs. This mechanistic parameter is related to the physical distress of transverse cracking that is visible at the pavement surface through calibrated curves that relate damage to distress. The model used to compute bottom-up and top- down cracking is based on computed fatigue damage and is presented as equation 8.

$$CRK_{TDorBU} = \frac{1}{1 + 1.0 \cdot FD^{C_3}_{TDorBU}} \quad (8)$$

where

$CRK_{TD\ or\ BU}$	=	predicted amount of bottom-up or top-down cracking (fraction)
$FD_{TD\ or\ BU}$	=	calculated fatigue damage (top-down or bottom-up)
C_3	=	calibration factor

Punchouts

A punchout is defined as the segment of PCC between two closely spaced cracks (typically 2 to 3 ft) where a longitudinal crack occurs (typically 3 to 5 ft from the slab edge). The longitudinal crack typically begins as micro-cracks at the top surface of the CRC overlay slab, coalesces as a longitudinal hairline crack with the application of repeated traffic loads, and finally propagates downward through the CRC slab to form a punchout.

Punchout prediction begins with computing the pavements critical structural responses—tensile bending stress in the top surface of the CRC in the transverse direction. This is followed by computing fatigue damage (computed using the critical structural responses and applied traffic). Fatigue damage is then used to compute punchouts. A detailed description of the punchout prediction procedure is presented in Part 3—DESIGN ANALYSIS, Chapter 4 and summarized in the following sections.

Fatigue damage is calculated incrementally to account for the effects of changes in traffic, PCC strength, and so on, on fatigue damage. The incremental approach leads to more accurate assessment of the accumulated fatigue damage, because the effects of the changes in material properties over time and seasons are considered directly in the damage calculation. The general expression for fatigue damage accumulations is as follows:

$$FD_{PO} = \sum \frac{n_{i,j,k}}{N_{i,j,k}} \tag{9}$$

where

FD_{PO} = accumulated fatigue damage over the design period (for the measured or computed mean crack spacing).

n_{ijk} = number of applied axle load applications of the j^{th} magnitude evaluated during the i^{th} traffic increment and the k^{th} temperature difference increment.

N_{ijk} = number of allowable axle load applications of the jth magnitude evaluated during the i^{th} traffic increment and the k^{th} temperature difference increment.

Note that an estimate of past fatigue damage is not required for bonded PCC over existing CRCP. This is because it is assumed that the existing CRCP is in relatively good condition and areas of localized distress are replaced with full-depth patching. In addition, the new PCC surface becomes the critical location for the critical stresses that cause punchpouts. The allowable number of load applications is computed using the maximum bending stresses (σ_{ij}) and bending strength for each design wheel load *(j)* for each time increment *(i)* using the following relation:

$$LogN_{ij} = C_1\left(\frac{MR}{\sigma_{totij}}\right)^{C2} \tag{10}$$

where

N_{ij} = number of allowable load applications during time increment i due to load of magnitude j

MR = PCC mean modulus of rupture

$\sigma_{tot\ ij}$ = total bending stress

C_1, C_2 = calibration constants

The model for punchout prediction as a function of accumulated fatigue damage due to slab bending in the transverse direction has the following functional form:

$$PO = \frac{C_3}{1 + C_4 FD_{PO}^{C_5}} \quad (11)$$

where

PO = total predicted number of punchouts per mile
FD = accumulated fatigue damage (due to slab bending in the transverse direction) at the end of the design life
C_3, C_4, C_5 = calibration constants

6.0 Comparison of Measured and Predictions Distress

The steps involved in comparing new PCC design model predictions of distress (for PCC rehabilitation design) and measured distress obtained from in-service PCC rehabilitated pavements were as follows:

1. Identify sources of data.
2. Database assembly.
3. Data quality assessment and estimation of missing data.
4. Run the 2002 Design Guide software and predict distress.
5. Perform statistical analysis (to determine suitability of using new PCC design models to predict PCC rehabilitated pavement distress).

Comparison of measured and predicted distress was done for all the different PCC rehabilitation design alternatives (see table 5) where data was available. A good fit between measured and predicted distress implies the new PCC design models could reasonably predict distress for PCC rehabilitated pavements without any significant modifications or recalibration.

Table 5. A summary of the distress models applicable to various PCC rehabilitation alternative.

Rehabilitation Type	Distress
Restoration of existing JPCP	• Faulting • Transverse cracking
Unbonded JPCP Overlay of existing rigid pavement	• Faulting • Transverse cracking
Unbonded CRCP Overlay of existing rigid pavement	• Punchout
Bonded PCC overlay of existing JPCP	• Faulting • Transverse cracking
Bonded PCC overlay of existing CRCP	• Punchouts
JPCP overlay of existing flexible/composite pavement	• Faulting • Transverse cracking
CRCP overlay of existing flexible/composite pavement	• Punchouts

However, if the fit of measured and predicted distress was inadequate, the new PCC design models would have to be recalibrated or redeveloped entirely. There were no data available for evaluating three PCC rehabilitation design alternatives, namely bonded PCC over existing JPCP, JPCP overlay over existing flexible pavement, and CRCP overlay over existing flexible pavement, and thus no analyses were conducted for these alternatives (see table 6). A thorough sensitivity analysis was, however, performed to establish the validity of using the new PCC design models for these PCC rehabilitation design alternatives.

Table 6. Methods used in model verification and calibration for different rehabilitation designs with PCC alternatives.

Rehabilitation Design With PCC Alternative	**Comparison of Model Distress Predictions to Observed Distress of In-Service Pavements**
Restoration of existing JPCP	✓
Unbonded JPCP Overlay of existing rigid pavement	✓
Unbonded CRCP Overlay of existing rigid pavement	✓
Bonded PCC overlay of existing JPCP	
Bonded PCC overlay of existing CRCP	✓
JPCP overlay of existing flexible/composite pavement	
CRCP overlay of existing flexible/composite pavement	

Identification of Sources of Data

Data from the LTPP database, ACPA Longevity and Performance of Diamond-Ground Pavements study, and NCHRP Project 10-41—Guidelines for the Design of Unbonded PCC Overlays were used in analysis (2, 3, 4). Figure 20 shows the location of the in-service test pavements used in analysis. A detailed description of the test sections is presented in table 7.

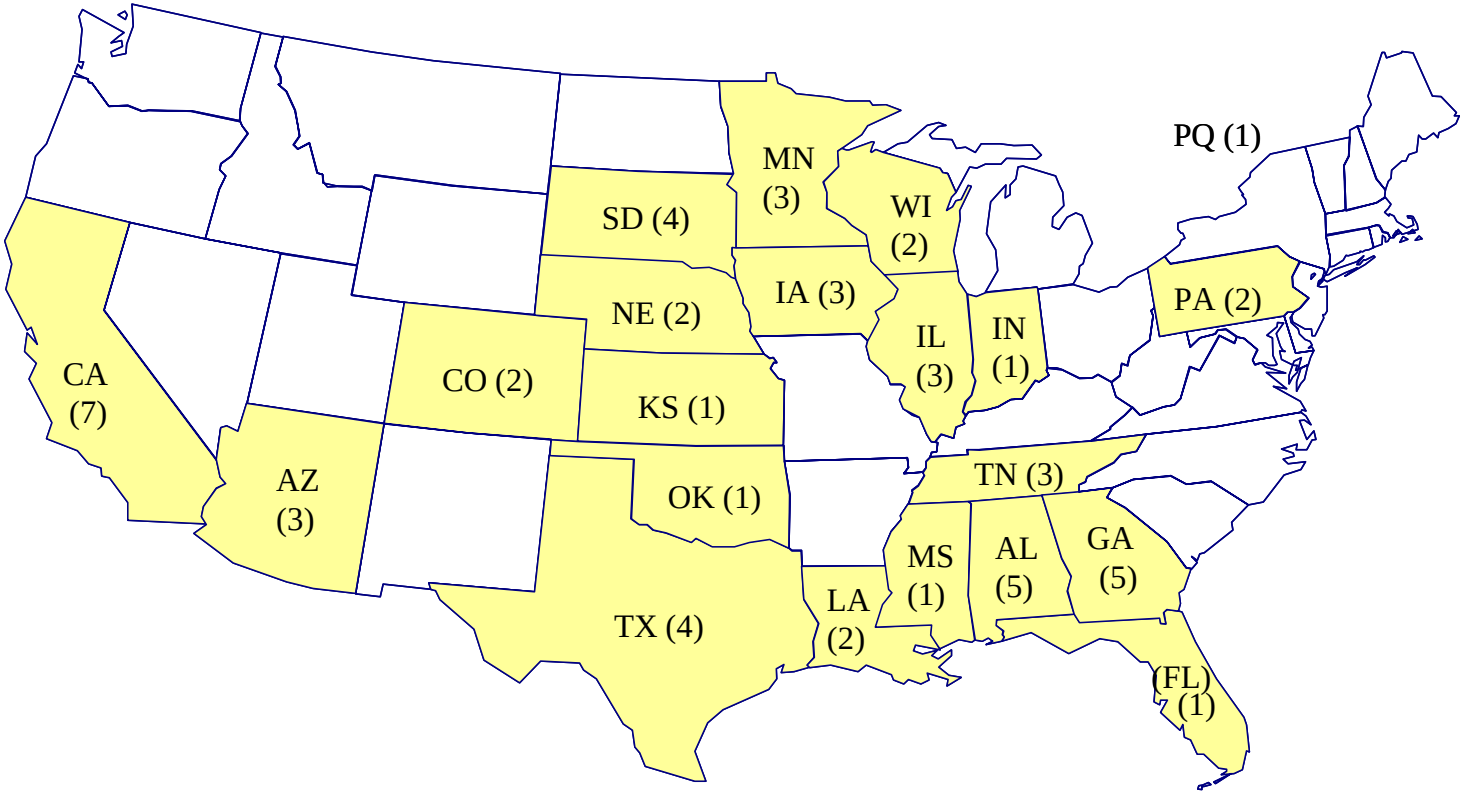

Figure 20. Summary of the number and location of test pavements used in calibration of rehabilitation design with PCC procedure.

Table 7. Description of test sections used in PCC rehabilitation verification, validation, and calibration.

SHRP_ID[1]	LTPP State Code	State	Rehabilitation Alternative	Section Length, ft	LTPP County Code	Functional Class	Direction of Travel	Milepoint	Elevation	Latitude (deg)	Longitude (deg)
0600	1	Alabama	Restored JPCP	500/1000	55	Rural Principal Arterial - Interstate	South	—	1335	34	85
0600	4	Arizona	Restored JPCP	500/1000	5	Rural Principal Arterial - Interstate	East	202.16	6900	35	111
0600	6	California	Restored JPCP	500/1000	93	Rural Principal Arterial - Interstate	North	14.58	1230	41	122
A600	29	Missouri	Restored JPCP	500/1000	113	Rural Principal Arterial - Interstate	West	0.54	13	38	121
0600	46	South Dakota	Restored JPCP	500/1000	13	Rural Principal Arterial - Other	West	308	1317	45	98
0600	47	Tennessee	Restored JPCP	500/1000	113	Rural Principal Arterial - Interstate	West	—	575	35	88
9048	6	California	Unbonded JPCP	500	73	Rural Principal Arterial - Interstate	East	33.44	2510	32	116
9049	6	California	Unbonded JPCP	500	113	Urban Principal Arterial (Freeways or Expressways)	West	0.54	13	38	121
9107	6	California	Unbonded JPCP	500	61	Rural Principal Arterial - Interstate	West	63.22	5641	39	120
9019	8	Colorado	Unbonded JPCP	500	123	Rural Principal Arterial - Interstate	North	246.5	4970	40	104
9020	8	Colorado	Unbonded JPCP	500	69	Rural Principal Arterial - Interstate	South	256.4	4550	40	104
4118	13	Georgia	Unbonded JPCP	500	207	Rural Principal Arterial - Interstate	South	183.4	750	33	83
9020	18	Indiana	Unbonded JPCP	500	53	Rural Principal Arterial - Interstate	South	66.47	860	40	85
9037	20	Kansas	Unbonded JPCP	500	177	Urban Principal Arterial	East	365.64	850	39	95
9075	27	Minnesota	Unbonded JPCP	500	129	Rural Principal Arterial - Other	North	103.13	1090	44	95
7012	28	Mississippi	Unbonded JPCP	500	149	Rural Principal Arterial - Interstate	West	13.7	156	32	90
6701	31	Nebraska	Unbonded JPCP	500	79	Urban Other Principal Arterial	North	69.59	1871	40	98
4155	40	Oklahoma	Unbonded JPCP	500	147	Rural Principal Arterial - Other	North	—	734	36	95
1627	42	Pennsylvania	Unbonded JPCP	500	33	Rural Principal Arterial - Interstate	West	—	1300	41	78

[1]Only 0600 test sections where diamond grinding was performed was used in verifying and validating new PCC design transverse joint faulting prediction model for restored JPCP. All 0600 test sections with transverse cracking data was however used in verifying and validating new PCC design transverse cracking prediction model for restored JPCP.

Table 7. Description of test sections used in PCC rehabilitation verification, validation, and calibration, continued.

SHRP_ID	State	LTPP State Code	Pavement Type	Section Length, ft	LTPP County Code	Functional Class	Direction of Travel	Milepoint	Elevation	Latitude (deg)	Longitude (deg)
3569	48	Texas	Unbonded CRCP over PCC	500	223	Rural Principal Arterial - Interstate	West	115.3	523	33	95
3845	48	Texas	Unbonded CRCP over PCC	500	97	Rural Principal Arterial - Interstate	South	—	762	33	97
9167	48	Texas	Unbonded JPCP over PCC	500	349	Rural Principal Arterial - Interstate	North	215.21	356	31	96
9355	48	Texas	Unbonded JPCP over PCC	500	139	Urban Principal Arterial - Interstate	South	407.6	635	32	96
9018	89	Quebec	Unbonded JPCP over PCC	500	5	Rural Principal Arterial - Other	West	3.2	52	46	4
0700	19	Iowa	Bonded PCC/CRCP	500	—	Rural Principal Arterial - Interstate	—	—	1116	42.3	93.5
0700	22	Louisiana	Bonded PCC/CRCP	500	—	Rural Principal Arterial - Interstate	—	—	15	30.15	91.0
0700	27	Minnesota	Bonded PCC/CRCP	500	—	Rural Principal Arterial - Interstate	—	—	903	46.75	96.5
GA-1*	13	Georgia	Unbonded CRCP over PCC	—	—	Rural Principal Arterial - Interstate	—	—	1001	34	84
GA-4*	13	Georgia	Unbonded CRCP over PCC	—	—	Rural Principal Arterial - Interstate	—	—	704	33	84
GA-5*	13	Georgia	Unbonded CRCP over PCC	—	—	Urban Principal Arterial (Freeways or Expressways)	—	—	1004	34	84
IL- 3*	17	Illinois	Unbonded CRCP over PCC	—	—	Rural Principal Arterial - Interstate	West	—	436	39	90
PA-5*	42	Pennsylvania	Unbonded CRCP over PCC	—	—	Rural Principal Arterial - Interstate	—	—	540	42	80
WI-1*	55	Wisconsin	Unbonded CRCP over PCC	—	—	Rural Principal Arterial - Interstate	—	—	920	44	91

*Obtained from NCHRP 10-41 reports.

Table 7. Description of test sections used in PCC rehabilitation verification, validation, and calibration, continued.

ID	State	Pavement Type	Section Length, ft	County	Functional Class	Direction of Travel	Milepoint	Elevation	Latitude (deg)	Longitude (deg)
AL-IH-20E-183.0	Alabama	Restored JPCP	480	Calhoun	Rural Principal Arterial - Interstate	East	183	—	34	—
AL-IH-59N-235.5	Alabama	Restored JPCP	500	Dekalb	Rural Principal Arterial - Interstate	North	235	—	35	—
CA-IH-8E-43.4	California	Restored JPCP	1010	Imperial	Rural Principal Arterial - Interstate	East	43.4	—	33	—
FL-IH-10E-214.7	Florida	Restored JPCP	540	Leon	Urban Principal Arterial - Interstate	East	214.7	—	30	—
GA-IH-16W-59.9	Georgia	Restored JPCP	600	Laurens	Rural Principal Arterial - Other	West	59.9	—	33	—
IA-IH-80W-87.7	Iowa	Restored JPCP	500	Adair	Rural Principal Arterial - Interstate	West	87.7	—	41	—
NE-IH-80W-420.1	Nebraska	Restored JPCP	510	Cass	Rural Principal Arterial - Interstate	West	420.1	—	41	—
SD-IH-29S-174.0	South Dakota	Restored JPCP	930	Codington	Rural Principal Arterial - Interstate	South	174	—	45	—
WI-IH-43N-2.7	Wisconsin	Restored JPCP	900	Rock	Rural Principal Arterial - Interstate	North	2.7	—	42	—

Restored JPCP

Data was obtained from the LTPP SPS-6—Rehabilitation of Jointed PCC Pavements experiments. The specific SPS-6 test sections used were—0601, 0602, 0605, or A601, A602, and A605. SPS-6 examines the effects of climate, amount and type of CPR performed, and traffic levels on future performance. CPR performed on the SPS-6 test sections ranged from do nothing to full-depth patching and retrofitting joints with dowels. Specific CPR treatments applied included:

- Crack sealing.
- Transverse joint sealing.
- Full depth transverse joint repair patch.
- Full depth patching of PCC pavement other than at joint.
- Partial depth patching of PCC pavement other than at joint.
- PCC slab replacement.
- AC shoulder restoration.
- AC shoulder replacement.
- Diamond grinding surface (all sections used in verifying faulting).
- Pressure grout subsealing.
- Joint load transfer restoration.

Unbonded (JPCP or CRCP) Overlays of Existing PCC

Data was obtained from the following databases:

- LTPP GPS-9—Unbonded PCC overlays on PCC pavements experiment.
- NCHRP Project 10-41—Development of Guidelines for the Design of Unbonded Concrete Overlays.

The LTPP GPS-9 and NCHRP Project 10-41 databases contain data collected from unbonded JPCP and CRCP overlays over existing PCC. The typical test section consisted on an unbonded JPCP or CRCP overlay (with a thickness of 5-in or greater) placed over an existing PCC. A separator layer was used to prevent bonding between the two PCC slabs. The existing PCC was constructed over a base/ subbase, and subgrade. Four test sections (all located in Georgia) were constructed without separator layers. They were considered unbonded since no special effort was made to bond the existing and overlay PCC slabs.

Bonded PCC over JPCP or CRCP Overlays

No useable data were available in the LTPP data base for bonded PCC/JPCP overlays. This was because the only SPS-7 experiment with bonded PCC/JPCP test sections had data that was not in a useable form. There were three SPS-7 experiments with bonded PCC/CRCP test sections. However, they did not contain enough data to enable a detailed analysis to be performed.

Overlay PCC and existing PCC slab shear bond strength was evaluated to determine if the PCC overlay and existing slab were truly bonded. Full bonding was defined as having minimum shear

bond strength of 200 psi. A summary of test results is presented in table 8. The results in table 8 shows that for all the test sections with data available shear bond strength was greater than 200 psi.

Table 8. Summary of shear bond strength for bonded PCC overlays.

SHRP_ID	State Code	Overlay PCC Thickness, in	Existing PCC Thickness, in	Core Cross Sectional Area, in^2	Max. Load, lbs	Number of Tests	Mean Shear Bond Strength, psi	Min. Shear Bond Strength, psi	Max. Shear Bond Strength, psi	Std. Dev.
0702	19	3.95	7.35	12.60	7530	2	600	510	690	127
0703	19	4.18	7.64	12.55	5674	5	452	340	570	99
0704	19	4.04	7.96	12.57	6154	7	489	320	660	132
0705	19	4.39	7.91	12.54	6930	7	554	295	990	266
0707	19	6.00	7.80	12.48	4710	2	377	364	390	18
0708	19	5.27	7.70	12.56	8630	3	687	400	920	264
0709	19	5.48	7.80	12.54	6775	4	540	390	770	185
0702	22	3.64	7.73	12.52	7318	6	585	318	1001	243
0703	22	3.79	7.68	12.58	10004	8	794	267	2033	617
0704	22	3.70	7.86	12.61	9687	8	767	307	1396	462
0705	22	3.96	7.56	12.61	9915	8	785	257	1679	541
0706	22	6.04	7.75	12.62	12379	5	978	302	1371	408
0707	22	5.78	8.20	12.57	3805	1	303	303	303	
0708	22	5.63	7.92	12.57	8883	3	706	318	956	341
0709	22	5.31	7.93	12.56	8207	7	653	264	1404	463
0702	27	3.68	7.83	13.82	10135	4	730	550	990	194
0705	27	3.40	8.40	13.79	7430	1	530	530	530	
0706	27	5.00	7.77	13.88	9033	3	647	550	700	84
0707	27	4.90	7.96	13.92	10118	5	724	610	810	75
0708	27	5.58	7.15	13.94	8560	4	610	520	780	123
0709	27	4.66	7.68	13.93	9306	10	663	550	870	115

Data for JPCP or CRCP Overlays over Existing Flexible Pavements

No data were available for JPCP and CRCP overlays over existing flexible pavements in the LTPP databse. There was, however, several new JPCP or CRCP constructed over AC treated or HMAC bases used in developing and calibrating the new JPCP and CRCP design models. Since the new JPCP/CRCP over HMAC or AC treated bases were very similar to JPCP/CRCP overlays over existing flexible pavements the new JPCP and CRCP design models were deemed reasonable for use. The new PCC design models were however, subjected to a comprehensive sensitivity analysis as described in section 7 of this appendix.

Database Assembly

The next step after identifying data sources was to assemble a database of selected test pavements with the required inputs for analysis. Data was retrieved specifically from the LTPP Information Management System (IMS) for experiments GPS-9, SPS-6, and SPS-7 and the NCHRP 10-41 project database.

The hierarchical approach described in Part 1—Introduction of the Design Guide provided guidance on what specific data was ideal for analysis (note that LTPP generally have different sources of data for any given data element). The advantage of this approach was that it provided a lot of flexibility for obtaining the input data. The hierarchical approach (levels 1 through 3) was employed with regard to traffic, design, and materials characterization inputs. The three levels of inputs are described as follows:

- Level 1—inputs can be thought of as "first class" and provide for the highest level of accuracy of inputs. Thus, inputs obtained using Level 1 procedures would have the lowest level of uncertainty or error. Level 1 material inputs require laboratory or field testing.
- Level 2—inputs typically would be user-selected data from an agency database or could be derived from a limited testing program, or could be estimated through correlations from other test data.
- Level 3—inputs provide the lowest level of accuracy. Inputs typically would be user-selected default values or typical averages for the region.

For a given test section, input data was obtained from a mix of levels (e.g., PCC modulus of rupture—Level 2, traffic load spectra—Level 2, and subgrade resilient modulus—Level 3). It is important to realize that no matter what level of input data is used computational algorithms for estimating pavement responses and distress remain exactly the same. Table 9 presents a generalized description of the hierarchial levels of data used in analysis. Additional details are presented in Appendix FF.

Data Quality Assessment and Estimation of Missing Data

Data Quality Assessment

Data from the selected LTPP experiments and the NCHRP 10-41 study were further prepared for analysis by performing the following:

- Checking the data for reasonableness and identifying outliers or erroneous data.
- Identifying missing data.
- Cleaning up the data to remove errors and outliers.
- Estimating missing data.

The first step in assessing data reasonableness was to perform a univariate analysis along with scatter plots for each data element to determine basic statistics such as mean, ranges, standard deviation, variance, and so on. The statistics were then evaluated for reasonableness. Bivariate analysis and bivariate plots showing trends between various data elements were also used to

determine if the test data were consistent with expected trends. Specific data (test results) that were inconsistent with established trends or had excessively high or low values were deemed to be outliers or erroneous.

The LTPP data required very little cleaning. This was because LTPP data is obtained from field and laboratory testing and other sources using well recognized testing protocols and data management tools. Also, they are stored in the LTPP IMS only after undergoing 5 different levels (A through E) of data quality checks. The LTPP data were detailed and mostly at levels 1 and 2. Data obtained from the NCHRP 10-41 project database were collected as part of that study directly from the State Highway Agencies (SHA). They were mostly at level 3 and required some cleaning up. Distress (time series) data that had some obviously erroneous data were removed and not used in analysis.

Table 9. Generalized description of the hierarchial levels of data used in verification/calibration.

Input Variable	**Description of the Hierarchial Levels**		
	Level 1	**Level 2**	**Level 3**
Depth of steel placement from pavement surface (for CRCP)	Data from the LTPP database or construction reports	—	Mid depth
Total longitudinal steel cross-sectional area as percent of PCC slab cross-sectional area (for CRCP)	Data from the LTPP data base or construction reports	—	0.63 percent
Diameter of longitudinal reinforcing steel (CRCP)	—	—	0.63 in.
Edge support (tied PCC, widened lane, slab width, etc.)	Data from the LTPP data base	—	—
Base erodibility index[1]	—	—	Based on material type
Traffic[2]	Number of axle applications and axle load distribution as obtained from the LTPP database	Estimates of AADT (truck) from the LTPP database	Estimates of AADT (truck) from other sources or databases
Subgrade[3]	Modulus of subgrade reaction is determined by backcalculating using FWD deflection test data	Determined from the resilient modulus of each foundation layer	Determined from regional or typical values obtained from historical agency data for design
Location (longitude, latitude, and elevation)	Obtained from LTPP database	—	Estimated from maps and other geographical databases
Depth to water table	—	—	• 10ft (annual precipitation > 20 in/yr) • 40ft (annual precipitation < 20 in/yr)
Unbound and HMAC layer material gradation	Obtained from LTPP database	—	Default values based on material type and description
PCC elastic modulus	Obtained from LTPP database	Correlations with strength test data	From default compressive strength of 5900 psi
HMAC or AC stabilized materials modulus	—	—	From assumed volumetric and binder properties

Table 9. Generalized description of the hierarchial levels of data used in verification/calibration, continued.

Input Variable	Description of the Hierarchial Levels		
	Level 1	Level 2	Level 3
Cementatious materials modulus	—	—	Default typical values obtained from literature
Unbound materials modulus	—	—	Default typical values obtained from literature
PCC age at opening to traffic	Data from the LTPP database or construction reports	—	Typical summer months of between June and September
Month opening to traffic	Data from the LTPP database or construction reports	—	Month of construction plus a month
Effective built-in temperature difference in PCC slab	N/A	N/A	-10 ^{o}F (from new pavement calibration)
Transverse joint spacing (for JPCP)	Data from the LTPP database or project files	—	—
Transverse joint sealant type (for JPCP)	Data from the LTPP database or project files	—	Liquid sealant
Dowel diameter and spacing (for doweled JPCP)	Data from the LTPP database or project files	—	—
Distance between lane edge stripe and outside dual tire	—	—	18 in
PCC flexural, compressive, and tensile strength	Obtained from LTPP database or project files	Correlations with strength test data	From default compressive strength of 5900 psi
HMAC or AC stabilized materials binder content	Obtained from LTPP database or project files	—	From default values
HMAC or AC stabilized materials void content	Obtained from LTPP database or project files	—	From default values
HMAC or AC stabilized materials asphalt grade	Obtained from LTPP database or project files	—	From default values

1. Erodibility was estimated in accordance with guidance provided in Part II—Chapter 3 of the Design Guide.
2. For levels 2 and 3 estimates of AADT were used with default load spectrum data for a specific functional class of highway.
3. For level 1 the input data is pavement deflections which are then used to backcalculate modulus of subgrade reaction. For level 2, resilient moduli may be obtained by running field tests for DCP (for a given month) or laboratory analysis (at the optimum moisture content) of bulk samples obtained from the existing pavement for CBR, R-Value, AASHTO soil classification, etc. and transforming them into resilient modulus through models/correlations. The resilient moduli are then transformed into an equivalent modulus of subgrade reaction value using the procedure described in PART 3, Chapter 4.

Estimation of Missing Data

The LTPP database was mostly complete while the NCHRP 10-41 database had significant amounts of missing data. Where the amount of missing data was large or the specific data element missing was key to the success of this analysis the test section was remove from the assembled database and not used in analysis. Otherwise estimates of the missing data were determined as follows:

- For LTPP sections, missing data were replaced with sublevel E LTPP test data (i.e., data that had not undergone complete QA/QC checks) or were replaced with inventory data (i.e., typical tests values obtained from State highway agencies [SHA]). Sublevel E data when available was preferred to inventory data.
- For both LTPP and NCHRP 10-41, missing time dependent data was estimated through backcasting or forecasting techniques using appropriate linear or non linear models and a baseline input data (e.g., converting long-term PCC compressive strength into 28-day PCC compressive strength or forecasting/backcast traffic volumes). Other types of missing data were estimated through the use of correlations between the missing data element and some baseline data element (e.g., obtaining flexural strength from compressive strength data). Where no baseline data was available missing data was estimated by reviewing construction reports and past research documents or by assuming typical regional or national values. Note that assumptions were made only for data elements that were not very sensitive to predicted outputs.
- None of the pavement test sections (LTPP SPS-6, SPS-7, GPS-9 and NCHRP 10-41) contained information on PCC coefficient of thermal expansion (CTE). Default coefficients of thermal expansion values based on PCC coarse aggregate type and project location was used to estimate this missing data element (see table 10).
- Backcalculated modulus of subgrade reaction data were available for some GPS-9 and NCHRP 10-41 test sections. However, none was available for SPS-6 and SPS-7. Modulus of subgrade reaction was used directly when available. Otherwise it was computed from the subbase/subgrade resilient moduli.
- None of the SPS-6 and NCHRP 10-41 test sections had level 1 traffic inputs (axle load distributions, and so on). Some GPS-9 test sections, however, had level 1 traffic data. For test sections without level 1 traffic data estimates of annual daily traffic (ADT) or average annual daily traffic (AADT) and percent trucks were used to estimate truck traffic volumes along with default axle load distributions and number of axles per truck values. Default axle load distributions were determined based on the highway functional class and expected traffic stream (see Part 2, Chapter 4 of the Design Guide).
- All the test sections used in analysis had geographic location (longitude, latitude, and elevation) data that were used in creating a virtual weather station for obtaining climate related data for analysis. A key input—depth to water table was, however, not available and was thus estimated based on the climate zone in which the test section was located (wet [mean annual precipitation greater than 20 in] = 10 ft, dry = 40 ft).
- Some NCHRP 10-41 test sections (Illinois and Pennsylvania) had no measured punchout distress data. Number of punchouts/mile was estimated using the amount of full-depth patching and failures measured and reported. The size of the typical patch used in repairing a punchout was estimated to be 120 ft^2 for a 12-ft lane.

Table 10. Default CTE for PCC materials.

State	Aggregate Type	Default CTE ^{o}F ($x10^{6}$)
Pennsylvania	Limestone	6.47
Georgia	Granite	5.74
Oklahoma	Limestone	5.38
Nebraska	Limestone	5.61
Mississippi	Chert	6.94
Quebec	Granite	5.97
Colorado	Granite	6.01
Indiana		6.00
Ohio	Limestone	5.44
Kansas	Limestone	6.24
Minnesota		6.42
Texas	Sandstone, limestone, Dolomite	4.4
California	Conglomerate	5.89
U.S.	—	5.5

Some key input data such as existing PCC condition for unbonded JPCP and CRCP overlays were not collected as part of the LTPP program. They had to be determined for all the test sections that required such inputs. The procedures used are presented in the next few sections.

SPS-6—Estimating Initial Transverse Cracking

Past transverse cracking (prior to JPCP restoration) for SPS-6 test sections 0601, 0602, and 0605 was determined by:

1. Reviewing distress survey maps of distress surveys conducted just prior to or just after restoration.
2. Reviewing distress data (including area of patching) just prior to or just after restoration.

Information gathered from the reviews were used to estimate the number of transverse cracks (all severities) present and the number of transverse cracks repaired (with full-depth repairs or slab replacement) before restoration.

It was assumed that large full-depth repairs were typically due to transverse cracking (especially for pavements with no history of material related deterioration) and also that distress surveys conducted within the first year of restoration to some extent reflected pavement condition at the time of restoration. Note that the evaluation of past repair was done carefully to avoid classifying repair used to repair distresses such as D-cracking, corner breaks as transverse cracking related.

A summary of the CPR techniques applied to the SPS-6 test sections used in analysis is presented in table 11. Table 12 explains the reasons for full depth repairs for the sections where full-depth repairs was applied and figure 21 presents an example of the distress survey maps used in estimating transverse cracking (existing and patched) prior to restoration. Estimates of initial transverse cracking are presented in table 13.

Table 11. Summary of the CPR techniques applied to the restores JPCP test sections used in calibration.

SHRP_ID	Do Nothing	Crack Sealing	Transverse Joint Sealing	Full Depth Transverse Joint Repair Patch	Full Depth Patching of PCC Pavement Other Than at Joint	Partial Depth Patching of PCC Pavement Other Than at Joint	PCC Slab Replacement	AC Shoulder Restoration	AC Shoulder Replacement	Grinding Surface	Pressure Grout Subsealing	Joint Load Transfer Restoration in PCC Pavements
1_0601									X (6/26/1998)			
1_0602			X (4/12/1998)	X (4/12/1998)					X (6/26/1998)	X (4/12/1998)		
1_0605			X (4/12/1998)	X (4/12/1998)					X (6/26/1998)	X (4/12/1998)		X (4/12/1998)
29_A601		X (7/2/1998)	X (7/2/1998)									
29_A602		X (6/23/1998)	X (6/23/1998)	X (6/23/1998)						X (6/23/1998)		
29_A605		X (6/23/1998)	X (6/23/1998)	X (6/23/1998)						X (6/23/1998)	X (7/1/1998)	
4_0601	X											
4_0602		X (7/24/1990)	X (7/24/1990)			X (7/12/1990)			X (7/24/1990)			
4_0605		X (7/25/1990)	X (7/25/1990)	X (7/25/1990)		X (7/25/1990)	X (7/25/1990)			X (8/20/1990)		X (7/25/1990)
46_0601								X (33871)				
46_0602		X (5/8/1992)		X (5/8/1992)			X (5/8/1992)			X (5/8/1992)		
46_0605		X (5/2/1992)		X (5/2/1992)			X (5/2/1992)			X (5/2/1992)		
47_0601			X (3/25/1996)				X (3/25/1996)		X (5/1/1996)			
47_0602			X (3/25/1996)	X (3/25/1996)			X (3/25/1996)		X (35186)	X (3/25/1996)		
47_0605			X (3/25/1996)	X (3/25/1996)			X (3/25/1996)		X (5/1/1996)	X (3/25/1996)		
6_0601	X											
6_0602		X (5/5/1992)	X (5/5/1992)	X (5/5/1992)			X (5/5/1992)			X (****)		
6_0605			X (5/12/1992)	X (5/12/1992)			X (5/12/1992)					

Table 11. Summary of the CPR techniques applied to the restores JPCP test sections used in calibration, continued.

SHRP_ID	Do Nothing	Full Depth Transverse Joint Repair Patch	Full Depth Patching of PCC Pavement Other Than at Joint	Partial Depth Patching of PCC Pavement Other Than at Joint	PCC Slab Replacement	AC Shoulder Restoration	AC Shoulder Replacement	Grinding Surface	Pressure Grout Subsealing	Joint Load Transfer Restoration in PCC Pavements
AL-IH-20E-183.0								X (1986)		
AL-IH-59N-235.5								X 1983)		
CA-IH-8E-43.4								X (1997)		
FL-IH-10E-214.7			X					X (1992)		
GA-IH-16W-59.9								X (1997)		
IA-IH-80W-87.7								X (1984)		
NE-IH-80W-420.1								X (1989)		
SD-IH-29S-174.0			X					X (1990)		
WI-IH-43N-2.7								X (1994)		

Table 12. Summary of the reasons for full depth repairs (for test sections where full-depth repairs were applied).

SHRP_ID	State Code	Construction No.	Date Complete	Date Began	Reason Primary	Reason Other
0602	6	2	5/5/1992	5/5/1992	Transverse cracking (PCC)	Long. cracking (PCC)
0603	6	2	5/12/1992	5/6/1992	Transverse cracking (PCC)	Long. cracking (PCC)
0605	6	2	5/12/1992	5/8/1992	Transverse cracking (PCC)	Long. cracking (PCC)
0605	47	1	4/30/1996	3/11/1996	Long. cracking (PCC)	Patch deterioration (PCC)
0601	47	1	4/30/1996	3/11/1996	Long. cracking (PCC)	Spalling (PCC)
0602	47	1	4/30/1996	3/11/1996	Patch deterioration (PCC)	TEST PIT
0605	4	2	7/25/1990	7/5/1990	Shattered or broken up slab	Transverse cracking (PCC)
0602	1	1	4/10/1998	4/8/1998	Slab settlement (PCC)	Transverse cracking (PCC)
0605	1	1	4/10/1998	4/8/1998	Slab settlement (PCC)	Transverse cracking (PCC)

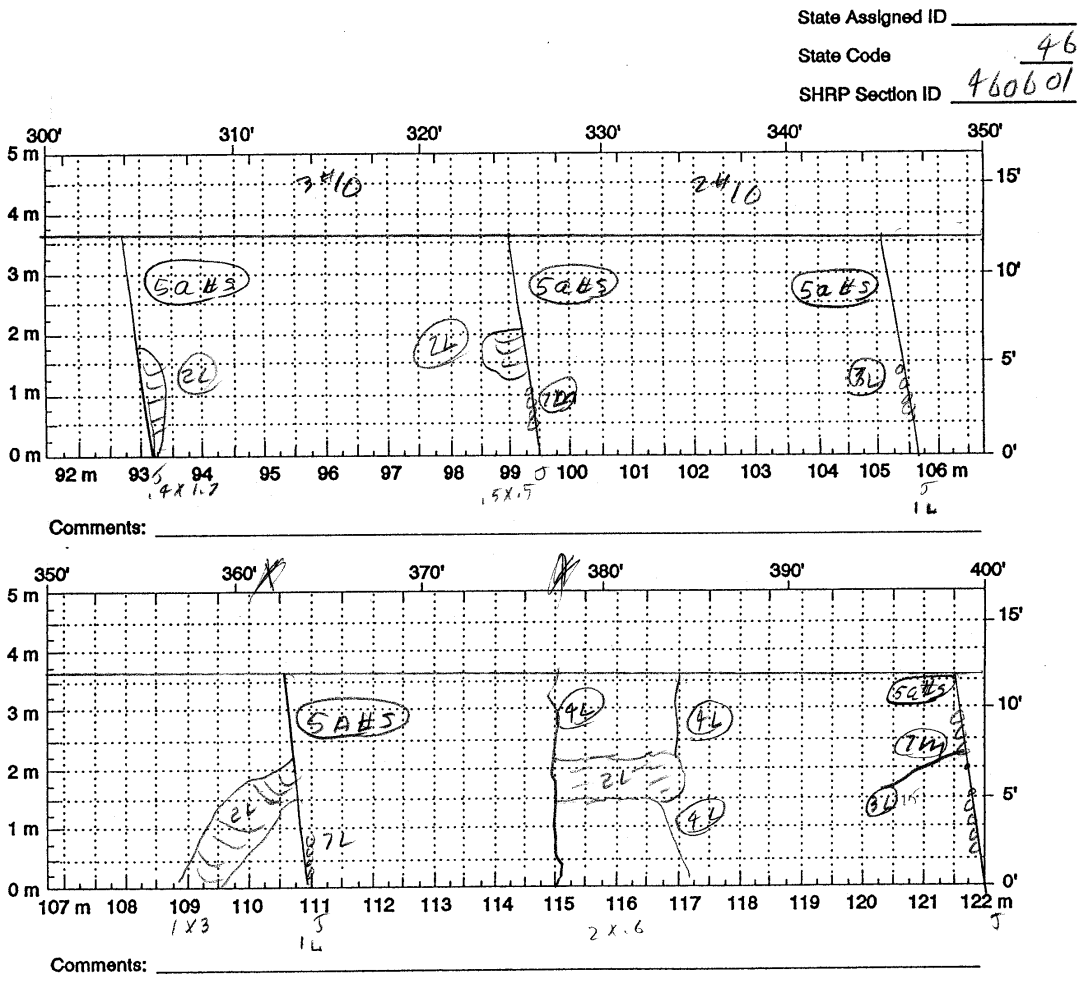

Figure 21. Example of distress map for test section 46_0601 (10-08-1992).

Table 13. Initial Cracking conditions for SPS-6 test sections.

State Code	SHRP ID	Section Length, ft	JTSP, ft	No of Slabs	No. of Transverse Cracks	Pct. Transverse Cracks	No of Initial Transverse Cracks	No of Repaired Cracks	Pct. Initial Transverse Cracks	Pct. Repaired Cracks
1	601	500	20	25	0	0.0	1	1	4.0	4
1	602	1000	20	50	0	0.0	2	1	4.0	2
1	605	1000	20	50	0	0.0	4	4	8.0	8
4	601	500	15	33	20	60.0	18	0	54.0	0
4	602	1000	15	67	33	49.5	30	0	45.0	0
4	605	1000	15	67	2	3.0	1.6	0	2.4	0
6	602	500	15.5	32	29	89.9	18	6	55.8	18.6
46	601	500	20	25	5	20.0	5	0	20.0	0
46	602	1000	20	50	1	2.0	2	2	4.0	4
46	605	1000	20	50	0	0.0	1	0.8	2.0	1.6
47	601	500	25	20	0	0.0	0.8	0.8	4.0	4
47	602	1000	25	40	1	2.5	0.8	0.8	2.0	2
47	605	1000	25	40	3	7.5	0.8	0.8	2.0	2
29	A601	500	30	17	13	78.0	11	0	66.0	0
29	A602	1000	30	33	7	21.0	7	0	21.0	0
29	A605	1000	30	33	3	9.0	1	0	3.0	0

GPS-9, SPS-7, and NCHRP 10-41 Data—Estimating Existing PCC Condition

Existing PCC layer condition data was not available for both the LTPP and NCHRP 10-41 study databases. However information pertaining to some preoverlay CPR was available in the NCHRP 10-41 project report for some test sections. This was used to assess the existing PCC layer condition as presented in table 14. For the test sections without pre-overlay condition information the following defaults were assumed:

- Unbonded overlays—existing pavement was in moderate to severe condition.
- Bonded overlays—existing pavement was in good to moderate condition.

Assigned conditions for such test sections are also presented in table 14. The assigned condition was used as the basis for selecting condition factors used for converting the laboratory test PCC elastic modulus (of intact material) to a design elastic modulus that reflects the condition of the entire PCC slab. The conditions factors applied were as follows:

- Good—0.75 to 1.0.
- Moderate—0.22 to 0.42.
- Severe—0.042.

Estimating Layer Moduli for Unbound and Cementatious Materials (All Data)

Layer moduli for unbound and cementatiously stabilized materials were estimated using the default values presented in table 15 based on material type description or AASHTO soil classification.

Table 14. Summary of preoverlay CPR for LTPP GPS-9, SPS-7, and NCHRP 10-41 test sections.

Data Source	State	County/ Nearby City	Highway	LTPP ID	Preoverlay Repair	Assigned Condition[1]
LTPP GPS-9 experiment	California	—	I-8	9048	—	Poor
	California	—	US-50	9049	—	Poor
	California	Cisco Grove	I-80	9107	Shattered slab replacement	Moderate
	Colorado	Carimer Counties/Weld	I-25	9019	Some slab removal/replacement	Moderate
	Colorado	Larimer County	I-25	9020	Some slab removal/replacement	Good
	Georgia			4118	—	Good
	Indiana	—	I-69	9020	—	Moderate
	Kansas	Topeka	US-24	9037	—	Poor
	Michigan	Ionia Co.	I-96	9029	Bituminous patching	
	Michigan	Dundee/Monroe Co.	US-23	9030	Bituminous patching	
	Minnesota	Adrian/ Nobles Co.	I-90	6300	—	
	Minnesota	Olivia	TH 71	9075	Patching of joints	Moderate
	Mississippi			7012	—	
	Mississippi		I-20	9030	—	Good
	Nebraska	Hall/Grand Island	US-281	6701	Full depth joint and panel repair	Moderate
	Ohio	Athens County	US-33	5569	Level slags with AC	
	Ohio	Clinton County	IR 71	9006	Underseal	
	Ohio	Franklin County	IR 270	9022	Full depth repairs of blowups	
	Oklahoma	—	US-75	4155	—	Good
	Pennsylvania	—	I-1	1627	—	Moderate
	Pennsylvania	Berg/Hamburg	I-78	9027	Replaced worst concrete areas with concrete patching	Good
	Quebec	—	State-30	9018	—	Moderate
	Texas	—	I-30	3569	—	Good
	Texas	—	I-35	3845	—	Good
	Texas	—	I-45	9167	—	Moderate
	Texas	—	I-35E	9355	—	Good
LTPP SPS-7 experiment	Iowa	—	—	19_0700	—	Good
	Louisiana	—	—	22_0700	—	Good
	Minnesota	—	—	27_0700	—	Good
	Missouri	—	—	29_0700[1]	—	
NCHRP 10-41 study	Georgia	Gwinnett	I-85	GA-1	CPR as needed	Good
	Georgia	Monroe	I-75	GA-4	None	Good
	Georgia	Gwinnett	I-85	GA-5	CPR as needed	Good
	Illinois	Madison	I-70	IL- 3	Limited patching	Moderate
	Pennsylvania	Erie	I-90	PA-5	Five percent patching	Poor
	Wisconsin	Jackson	I-94	WI-1	Patching	Poor

1. Based on the description available, DOT practices, and engineering judgment.

Table 15. Default layer moduli for unbound and cementatiously stabilized base and subbase materials.

Material Type/AASHTO Class	Default Modulus, psi
Lime stabilized material	50000
Cement stabilized material	300000 to 700000
Lean concrete material	2000000
A-1-a	40000
A-1-b	38000
A-2-4	32000
A-2-5	28000
A-2-6	26000
A-2-7	24000
A-3	29000
A-4	24000
A-5	20000
A-6	17000
A-7-5	12000
A-7-6	8000

Computation of Pavement Responses and Distress

The 2002 design guide software was used for computing all relevant pavement responses such as LTE, DE, fatigue damage, and crack width as well as distress over the age of the existing pavement. The model coefficients used to compute distress are summarized in tables 17 through 19. All of the coefficients were adopted from the calibrated distress models for new design were found to be acceptable with the exception of the model coefficients for the restored JPCP (including diamond grinding) transverse joint faulting prediction model. Here a modified set of model coefficients was used to account for the differences in the development and progression of transverse joint faulting for new and restored PCC.

Table 17. Model calibration coefficients for predicting mean transverse joint faulting for PCC rehabilitation design alternatives.

Model Coefficients	PCC Rehabilitation Design Alternatives			
	Restored* JPCP	Unbonded JPCP over Existing PCC	Bonded PCC over Existing JPCP	JPCP over Existing Flexible Pavement
C_1	0.934	1.129	1.129	1.129
C_2	0.6	1.1	1.1	1.1
C_3	0.001725	0.001725	0.001725	0.001725
C_4	0.0004	0.0008	0.0008	0.0008
C_5	250	250	250	250
C_6	0.4	0.4	0.4	0.4
C_7	0.65	1.2	1.2	1.2
C_8	400	400	400	400

*Modified model coefficients.

Table 18. Model calibration coefficients for predicting mean transverse cracking for PCC rehabilitation design alternatives.

Model Coefficients	PCC Rehabilitation Design Alternatives			
	Restored JPCP	Unbonded JPCP over Existing PCC	Bonded PCC over Existing JPCP	JPCP over Existing Flexible Pavement
C_1	2	2	2	2
C_2	1.22	1.22	1.22	1.22
C_3	-1.68	-1.68	-1.68	-1.68

Table 19. Model calibration coefficients for predicting punchouts for PCC rehabilitation design alternatives.

Model Coefficient	PCC Rehabilitation Design Alternatives		
	Unbonded CRCP over Existing PCC	Bonded PCC over Existing CRCP	CRCP over Existing Flexible Pavement
C_1	2	2	2
C_2	1.22	1.22	1.22
C_3	105.26	105.26	105.26
C_4	4	4	4
C_5	-0.38158	-0.38158	-0.38158
C_6	1	1	1

Statistical Analysis

STATISTICA was used in statistical analysis which consisted of the following:

1. Determining the correlation (coefficient of determination, R^2) between the measured and predicted distress for each distress type (for all PCC rehabilitation alternatives).
2. Determining the residual error (difference between predicted and measured distress) for each distress type.
3. Testing the data for independence using plots of residual error versus predicted distress for each distress type.
4. Determining whether there is a significant difference in measured and predicted distress using paired t-test by testing the following hypothesis;
    a. Null hypothesis, H_o: There is no significant difference in measured and predicted distress values?
    b. Alternative hypothesis, H_A: There is a significant difference in measured and predicted distress values?

In the paired t-test the null hypothesis is that the average of the differences between the paired observations (measured and predicted distress) is zero. STATISTICA computes the summary statistics of measured and predicted distress followed by the mean of the differences between the paired observations (i.e., measured and predicted distress), the standard deviation of these differences, and the 95 percent confidence interval for the mean. This is followed by computing the result of the null hypothesis test (p-value). If the calculated p-value is less than the predetermined level of significance (e.g., 5 percent or 0.05) the conclusion is that the mean difference between the paired observations is statistically significantly different from 0. Plots of

measured versus predicted distress showing the strength of the correlation between them and predicted distress versus the residuals (differences in predicted and measured distress) are presented in figures 22 through 27. A summary of the results of the pair t-tests (hypothesis testing) is presented in table 20.

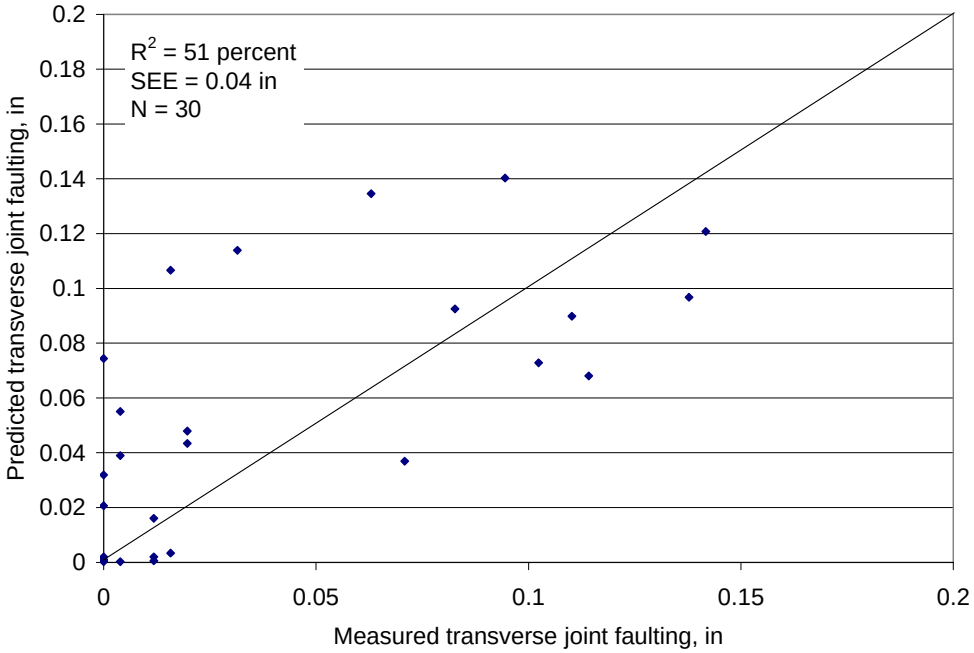

Figure 22. Plot of measured versus predicted mean transverse joint faulting (unbonded JPCP overlay over existing PCC).

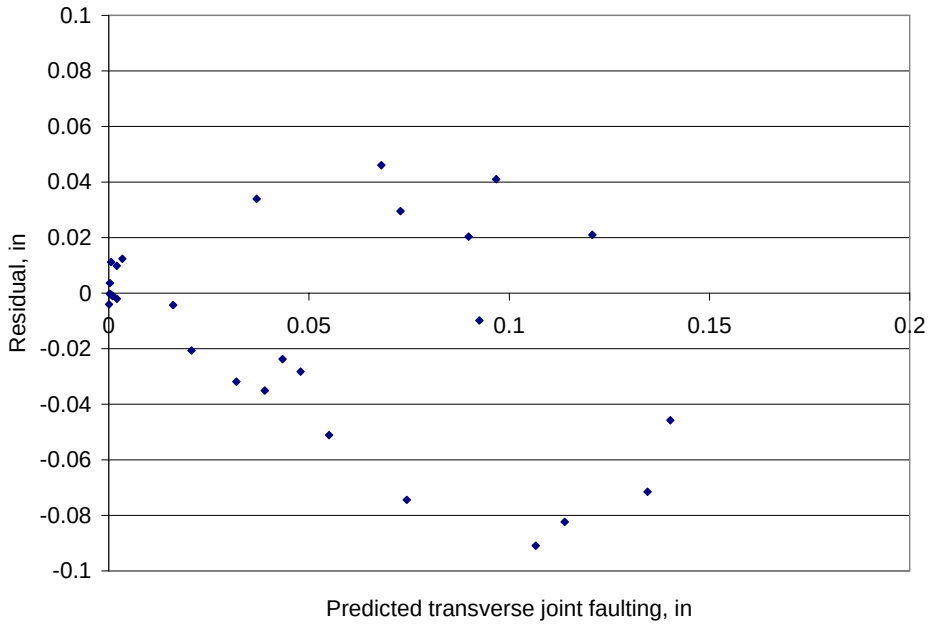

Figure 23. Plot of predicted mean transverse joint faulting versus residual (unbonded JPCP overlay over existing PCC).

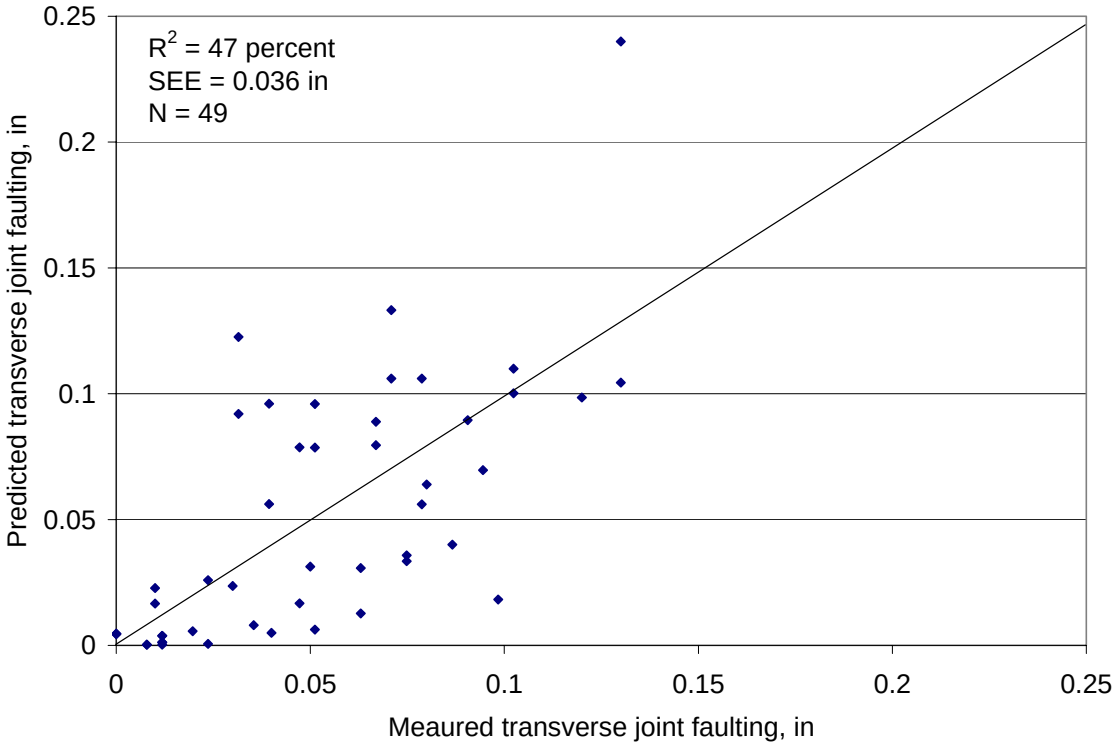

Figure 24. Plot of measured versus predicted mean transverse joint faulting (restored JPCP).

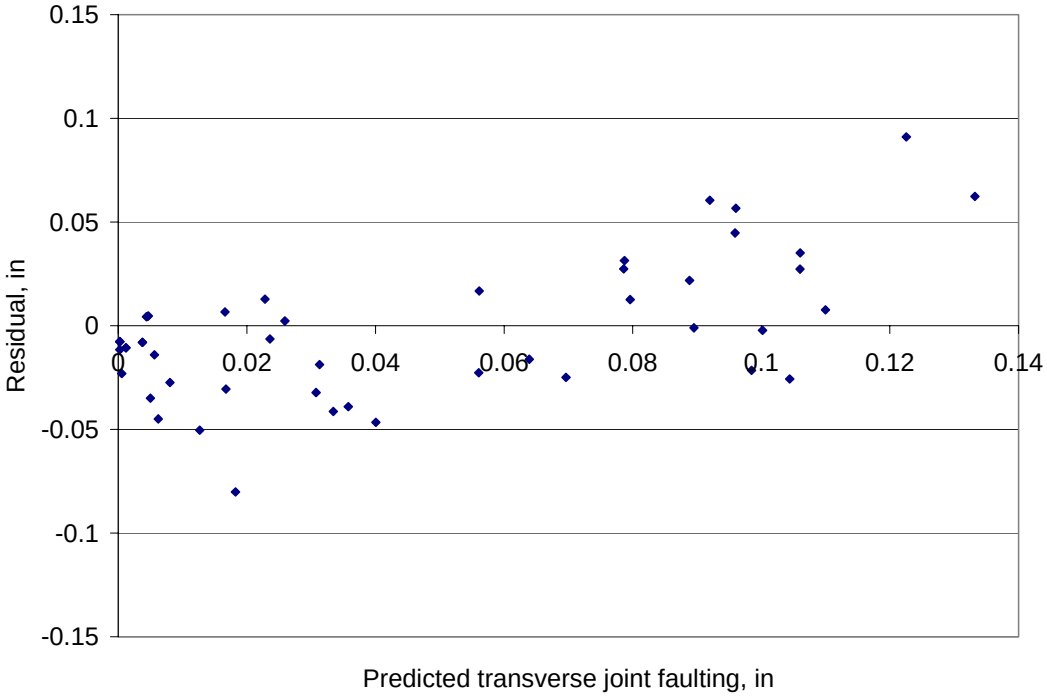

Figure 25. Plot of predicted mean transverse joint faulting versus residual (restored JPCP).

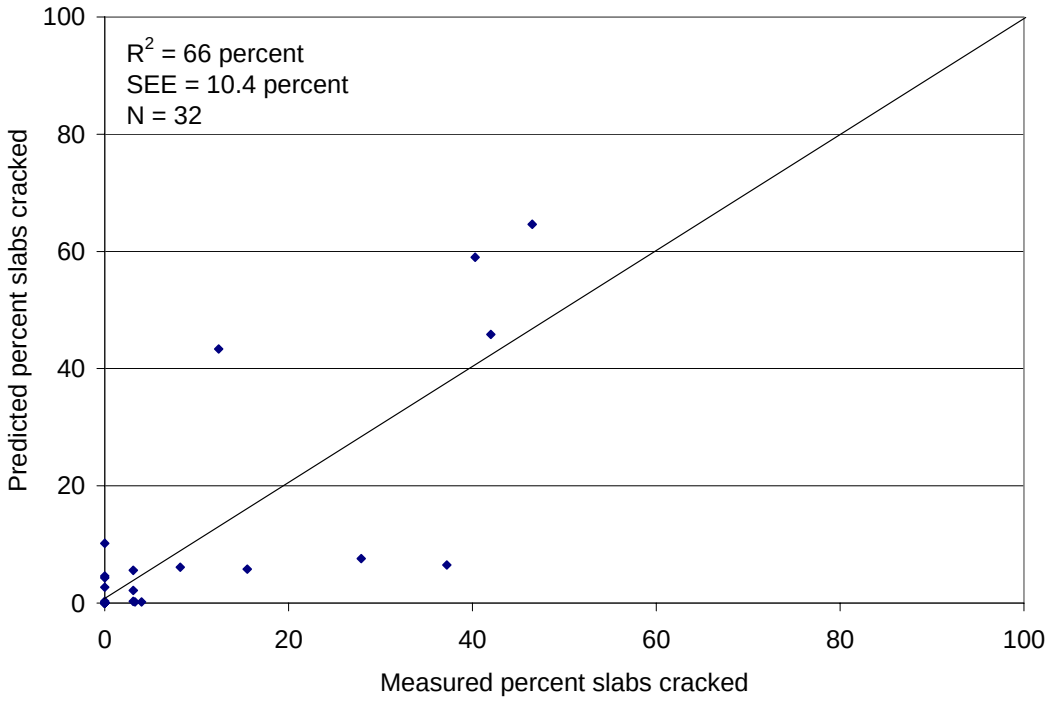

Figure 26. Plot of measured versus predicted percent slabs cracked (unbonded JPCP overlay over existing PCC).

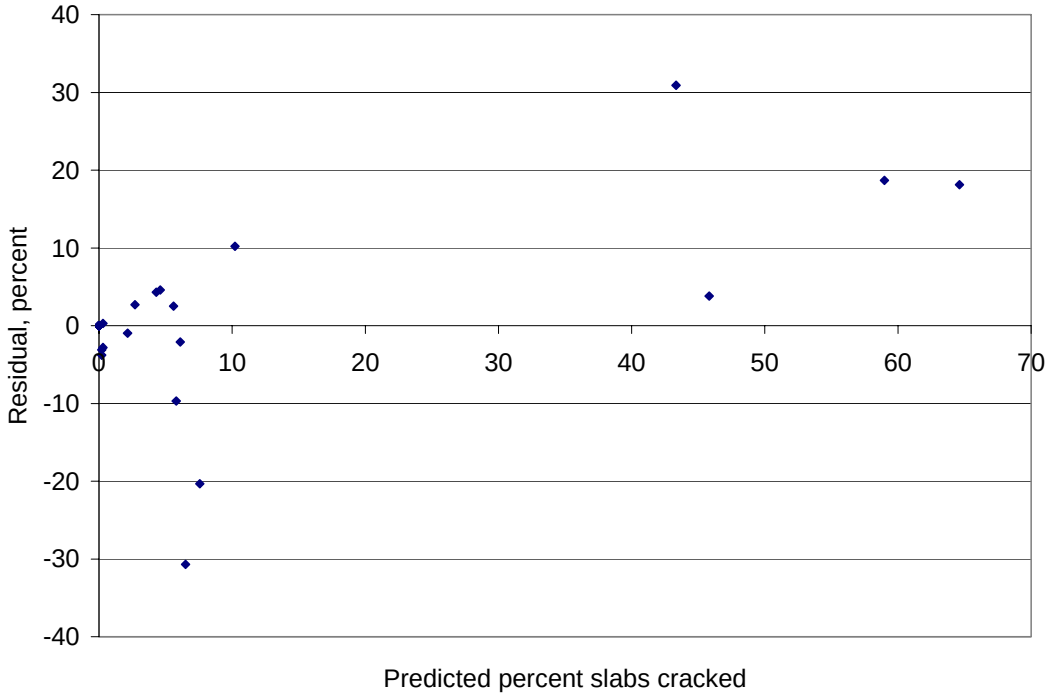

Figure 27. Plot of predicted percent slabs cracked versus residual (unbonded JPCP overlay over existing PCC).

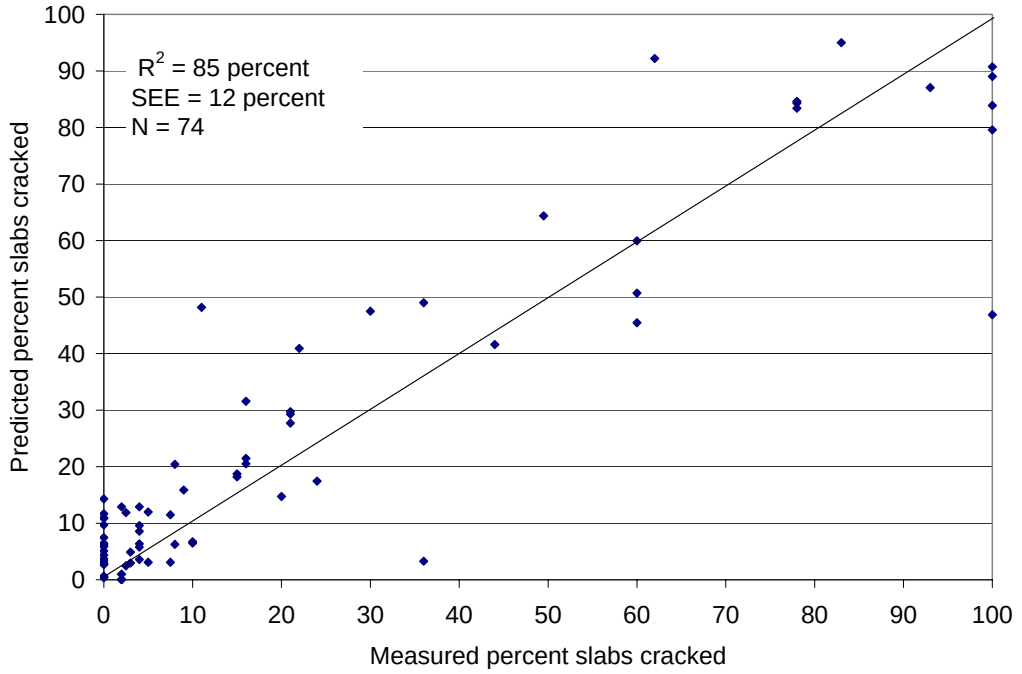

Figure 28. Plot of measured versus predicted percent slabs cracked (restored JPCP).

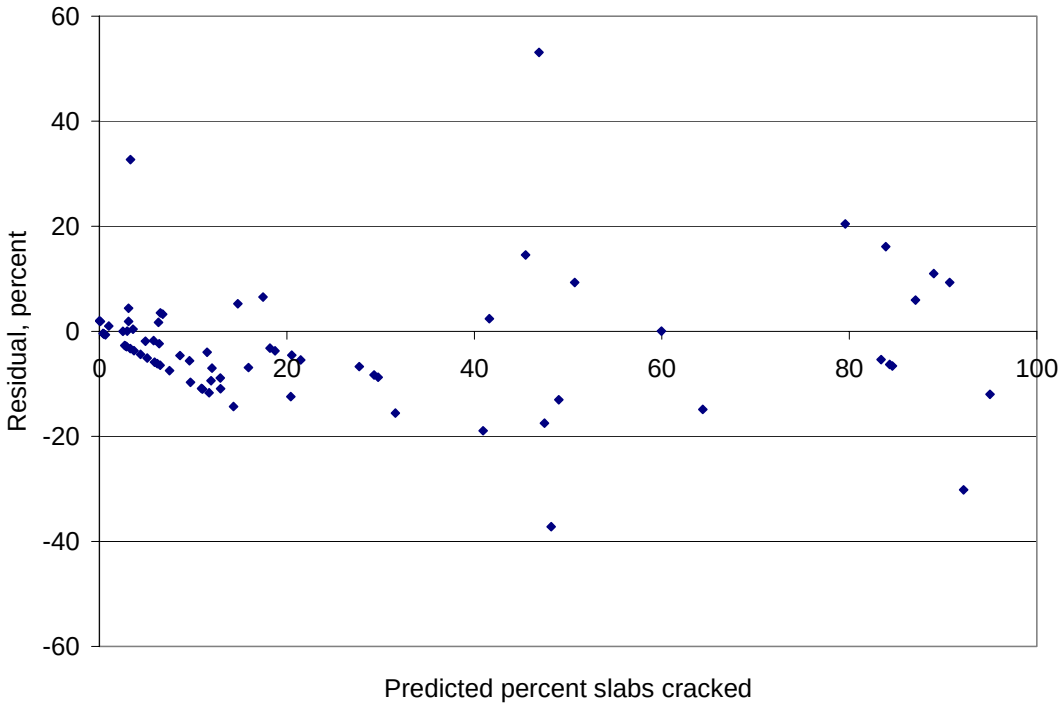

Figure 29. Plot of predicted percent slabs cracked versus residual (restored JPCP).

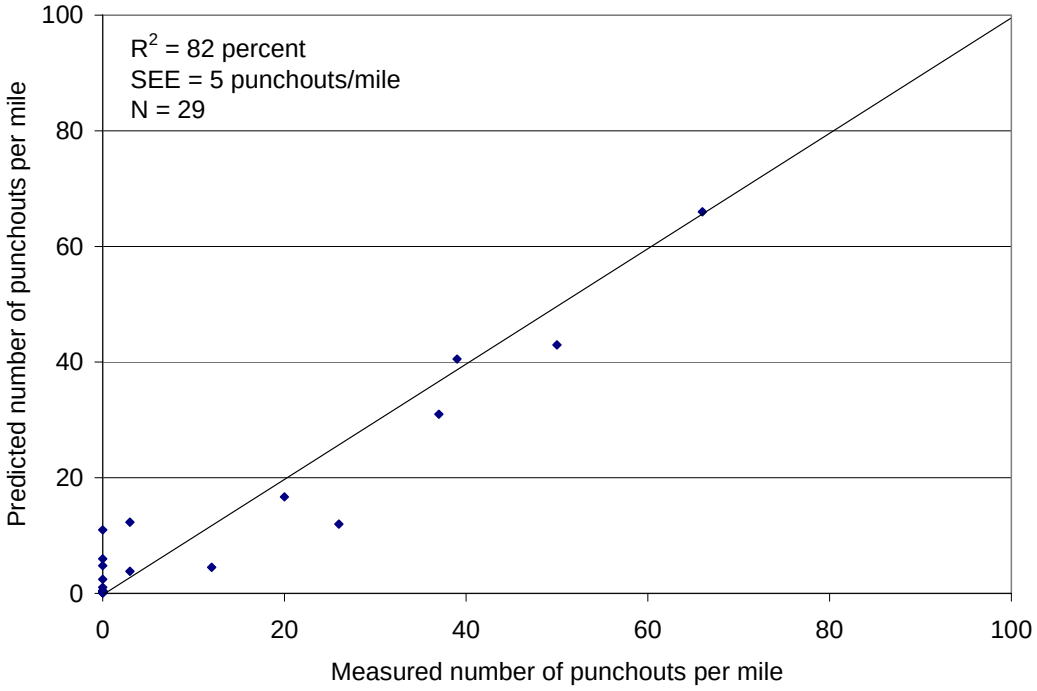

Figure 30. Plot of measured versus predicted number of punchouts per mile (unbonded CRCP overlay over existing PCC).

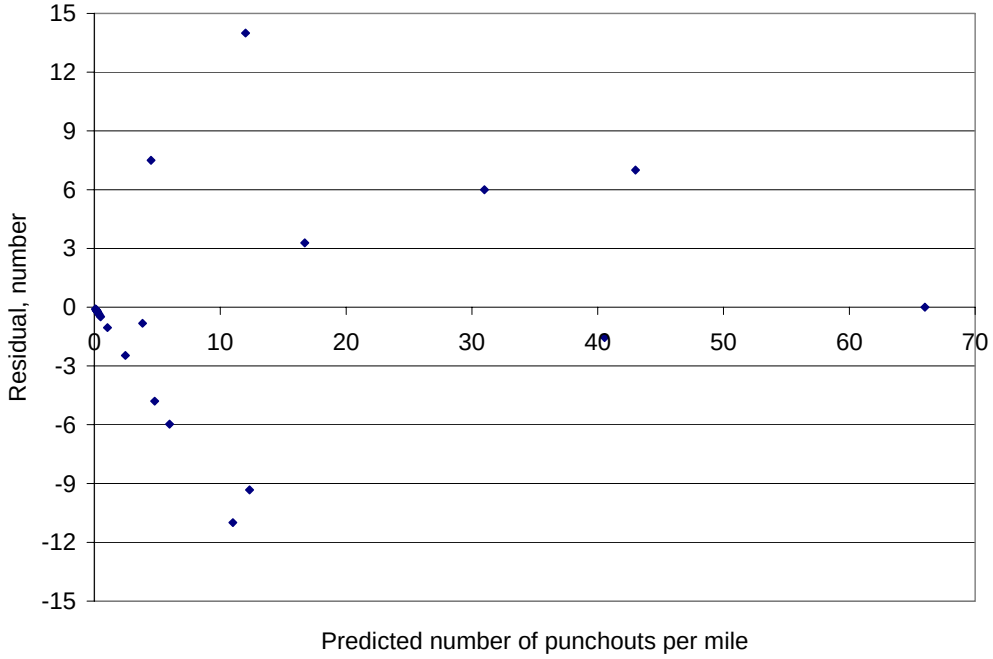

Figure 31. Plot of predicted percent slabs cracked versus residual (unbonded CRCP overlay over existing PCC).

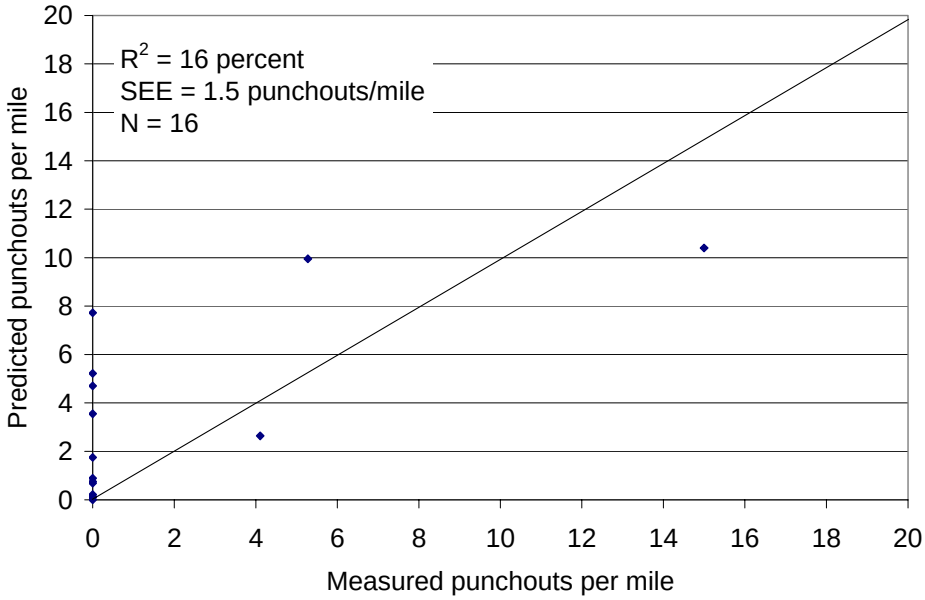

Figure 32. Plot of measured versus predicted number of punchouts per mile (bonded PCC over existing CRCP).

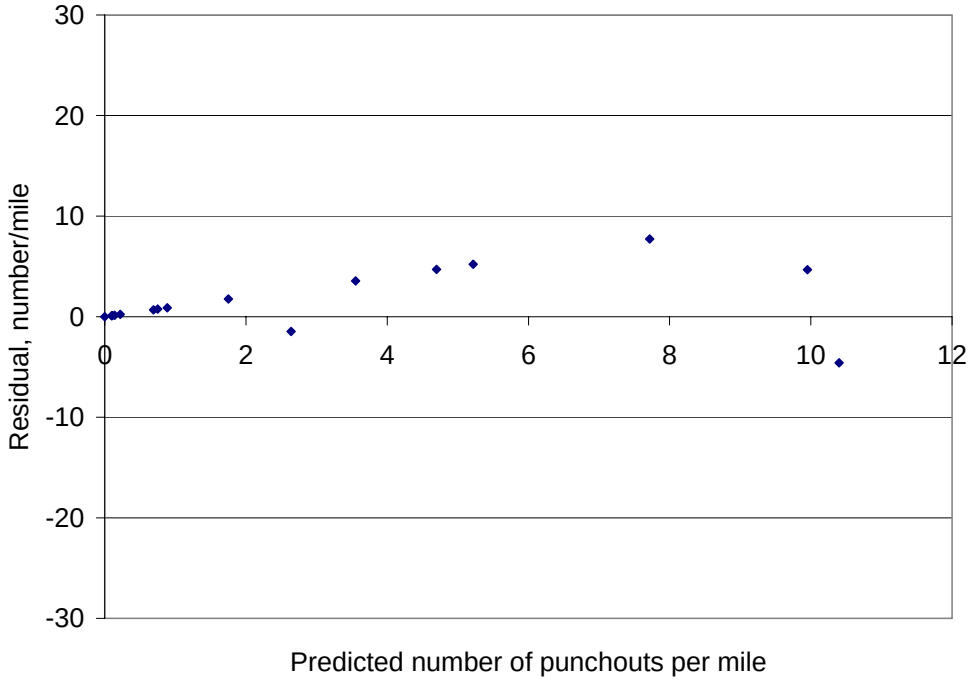

Figure 33. Plot of predicted percent slabs cracked versus residual (bonded PCC over existing CRCP).

Table 20. Summary of ANOVA results.

Distress Type	PCC Rehabilitation Alternative	Number of Data Points	Mean Distress Value		P-value	Is There a Significance Difference in Measured and Predicted Distress?
			Measured	Predicted		
Transverse joint faulting	Restored JPCP	47	0.046	0.049	0.54	No
	Unbonded JPCP over existing PCC	27	0.033	0.042	0.21	No
	Bonded PCC over existing JPCP[2]	—	—	—	—	—
	JPCP overlay over existing flexible pavement[2]	—	—	—	—	—
Transverse cracking	Restored JPCP	74	25.35	22.68	0.23	No
	Unbonded JPCP over existing PCC	32	8.4	7.7	0.69	No
	Bonded PCC over existing JPCP[2]	—	—	—	—	—
	JPCP overlay over existing flexible pavement[2]	—	—	—	—	—
Punchouts	Unbonded CRCP over existing PCC	29	8.8	8.9	0.91	No
	Bonded PCC over existing CRCP[1]	—	—	—	—	—
	CRCP overlay over existing flexible pavement[2]	—	—	—	—	—

[1]Insufficient data.
[2]Data not available.

The results presented in figures 22 through 33 shows that there was adequate correlation between the predicted and measured distress (R^2 ranges from 47 to 85 percent) with reasonable levels of error (MSE) between measured and predicted distress for all three distress types (faulting = 0.04 in, transverse cracking = 12 percent, punchouts = 5/mile). The plots of predicted distress versus residuals also showed no appreciable trends implying that the data used in analysis was independent. The results in table 18 show that there was no significant difference in predicted and measured distress for all the three distress types and for the different rehabilitation alternatives. This indicates that the model outputs not only correlated well with observed distress but predicted similar distress values as measured distress.

6.0 Sensitivity Analysis (Test Model over Range of Input Parameters)

The distress prediction models were further tested by performing a comprehensive sensitivity analysis to determine the effect of key inputs (see table 21) on predicted distress. The results are presented in figures 34 through 62 in the following sections for the different distress types for the 7 PCC rehabilitation alternatives.

Table 21. Key input values and levels used in sensitivity analysis.

Key Input Variables	Mean value	Range	
		Minimum	Maximum
Overlay PCC thickness (unbonded), in	8	6	10
Overlay PCC thickness (bonded), in	6	4	8
Overlay PCC 28-day flexural strength, psi	650	400	900
Overlay PCC CTE, per in	5.5	4.0	7.0
JPCP or CRCP over existing flexible pavement existing HMAC condition (percent cracking)	Moderate	Poor	Good
Unbonded JPCP or CRCP existing PCC condition (percent cracking)	Moderate	Poor	Good
Unbonded JPCP or CRCP existing PCC separation layer thickness, in	2	1	3
Cracking and repair prior to JPCP restoration, percent cracking	Moderate	Poor	Good
Shoulder	Tied PCC shoulders versus others		
Widened lane	12	14	14
JPCP dowel diameter, in	0	1	1.5
JPCP joint spacing, ft	15	16	20
CRCP steel content, percent steel	0.7	0.6	0.8

Restored JPCP

The goal was to determine the effect of CPR on a typical JPCP by predicting their effect on future distress. The specific CPR considered was:

- Diamond grinding (to reduce transverse joint faulting).
- Full-depth patching to repair transverse cracking.
- Transverse joint load transfer restoration/full-depth joint repair.
- Shoulder replacement with tied PCC shoulders.
- Widening of existing outer lanes.

The effects of these CPR on future transverse joint faulting and transverse cracking of existing deteriorated JPCP are presented in the following sections.

Transverse Joint Faulting

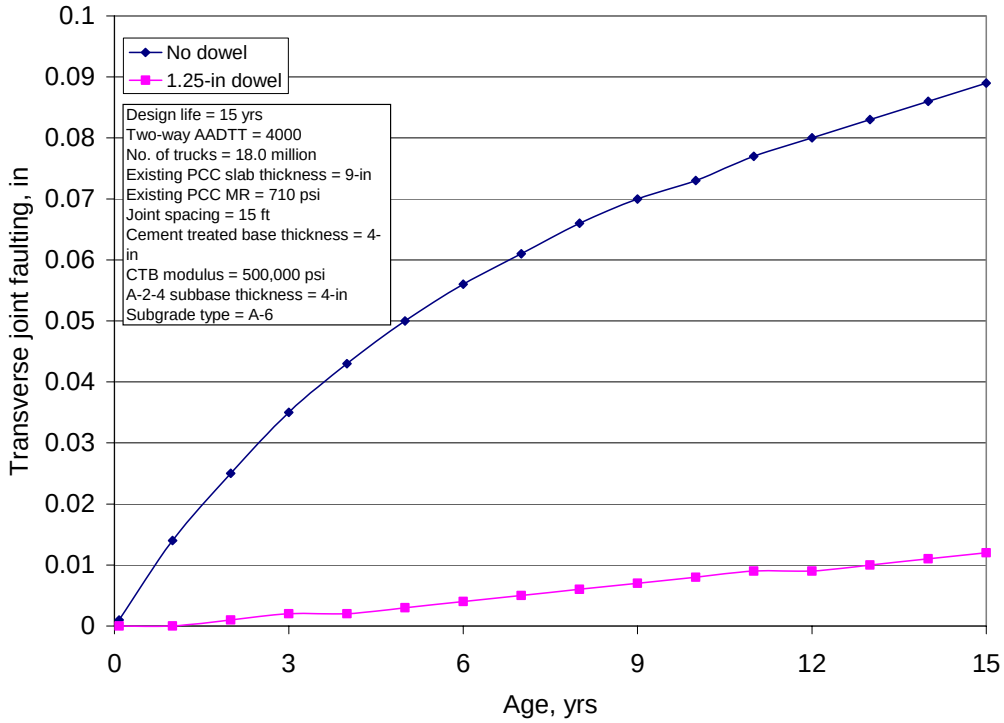

Figure 34. Plot showing the effect of LTR (dowel diameter 0, 1.0, 1.25, 1.5-in) on transverse joint faulting.

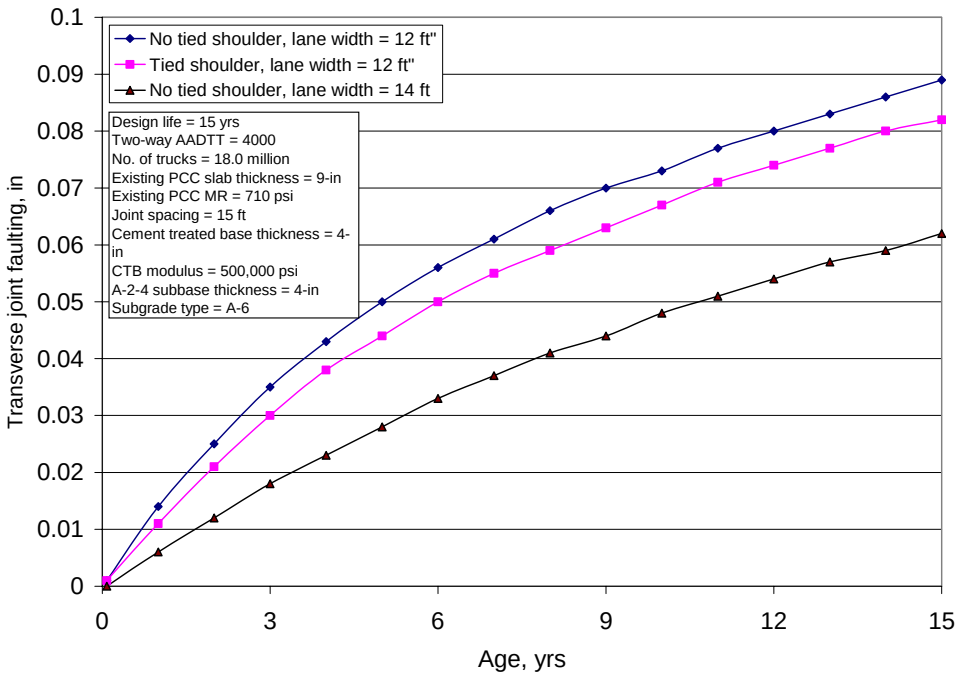

Figure 35. Plot showing the effect of retrofit shoulder (tied PCC or otherwise) and the effect of widened lane (existing lane=12ft and widened lane=14 ft) on transverse joint faulting.

Transverse Cracking

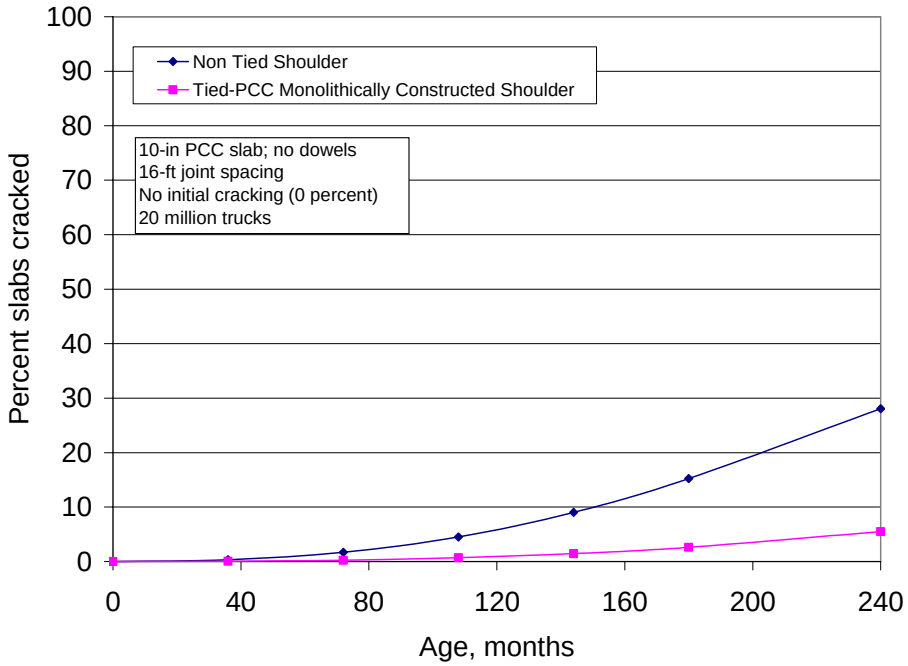

Figure 36. Plot showing the effect of edge support (use of tied PCC shoulders monolithically placed with the JPCP overlay traffic lane or retrofitted to existing JPCP or non tied PCC shoulder) on transverse cracking of restored JPCP.

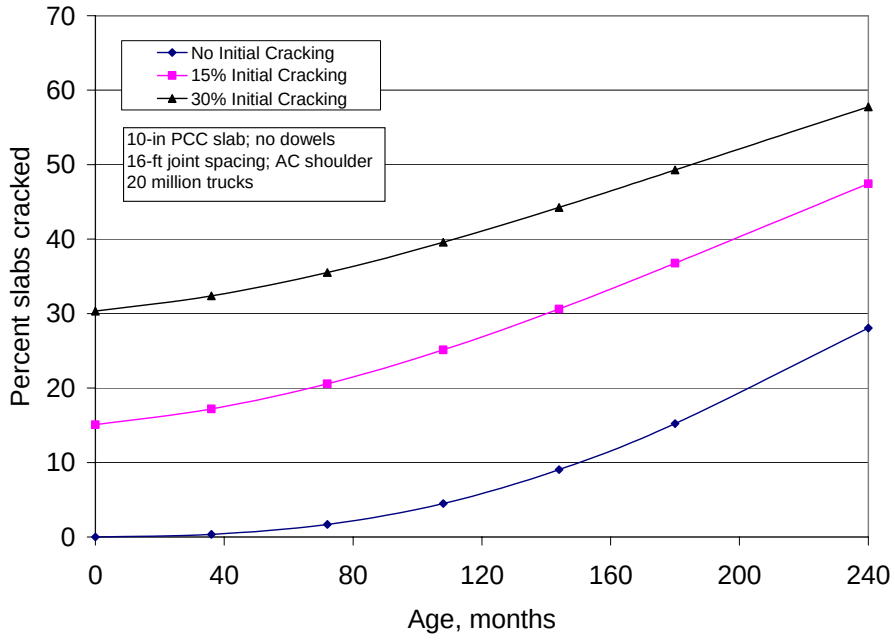

Figure 37. Plot showing the effect of existing JPCP transverse cracking (initial damage) on transverse cracking of restored JPCP.

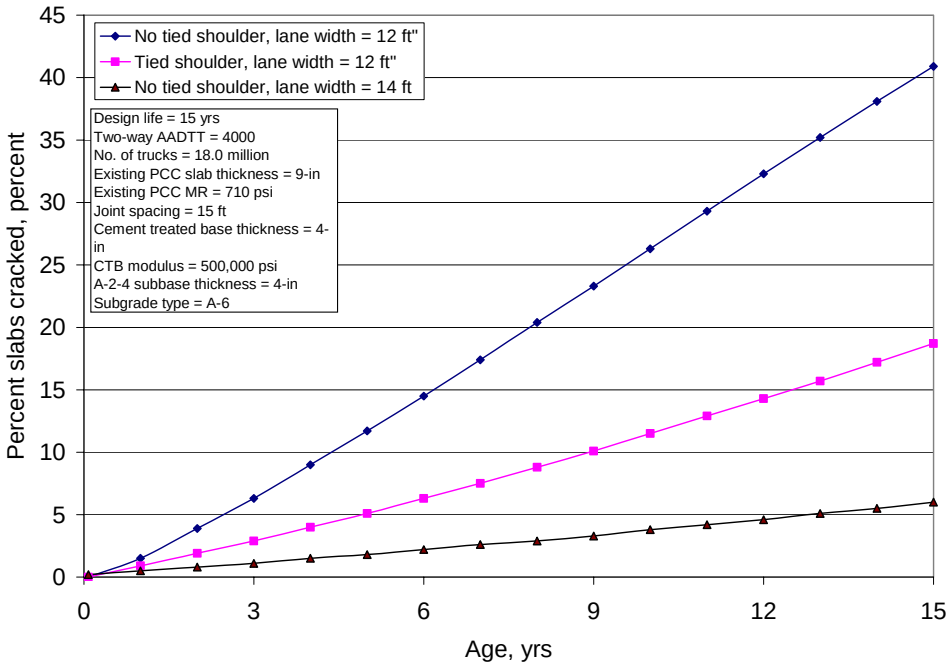

Figure 38. Plot showing the effect of retrofit shoulder (tied PCC or otherwise) and the effect of widened lane (existing lane 12ft, widened lane 13 ft, widened lane 14 ft) on transverse cracking.

Unbonded JPCP over Existing PCC

Transverse Joint Faulting

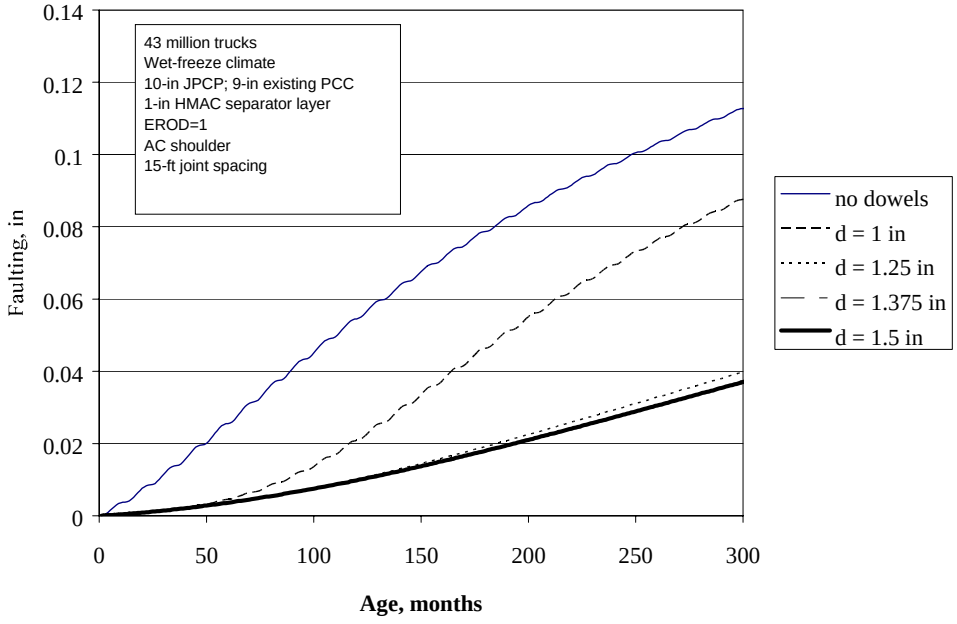

Figure 39. Plot showing the effect dowel diameter on predicted mean transverse joint faulting (for unbonded JPCP overlays).

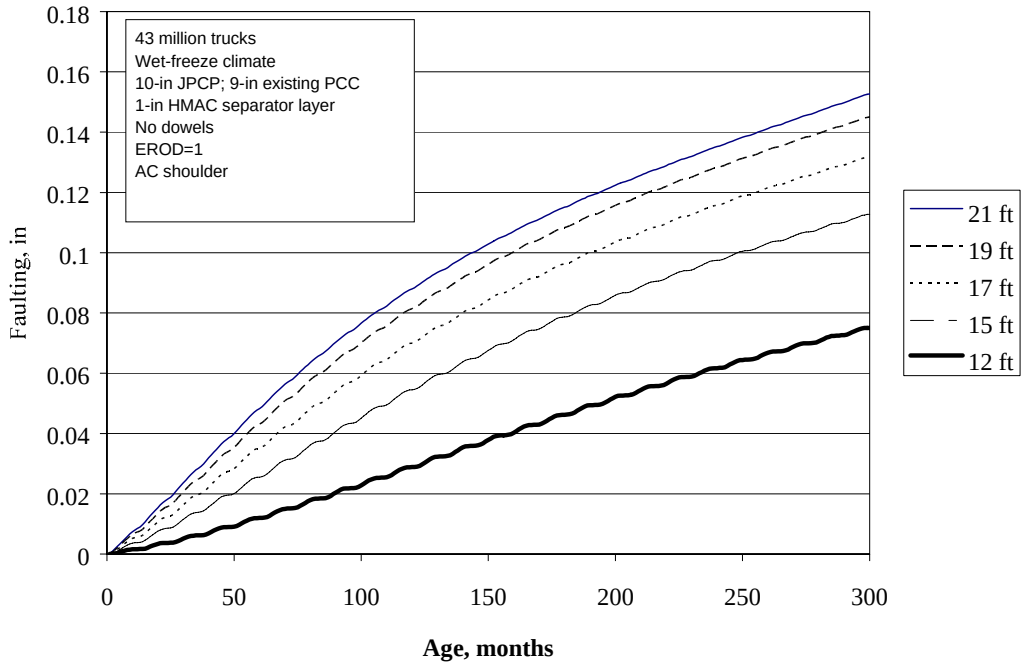

Figure 40. Plot showing the effect of joint spacing on predicted mean transverse joint faulting (for unbonded JPCP overlays).

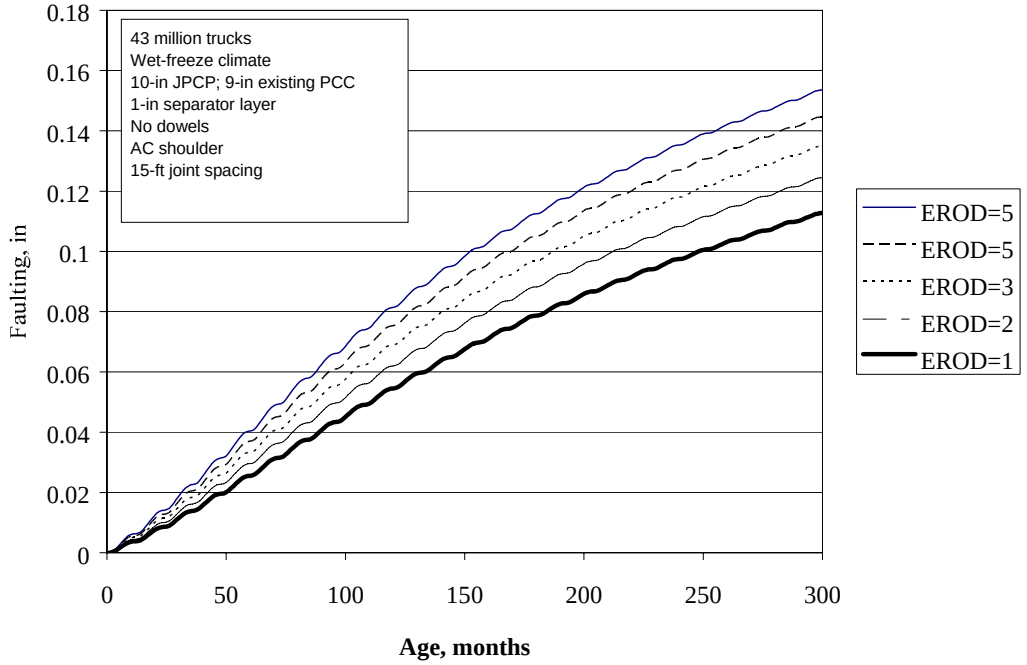

Figure 41. Plot showing the effect of separator layer erodibility on predicted mean transverse joint faulting (for unbonded JPCP overlays).

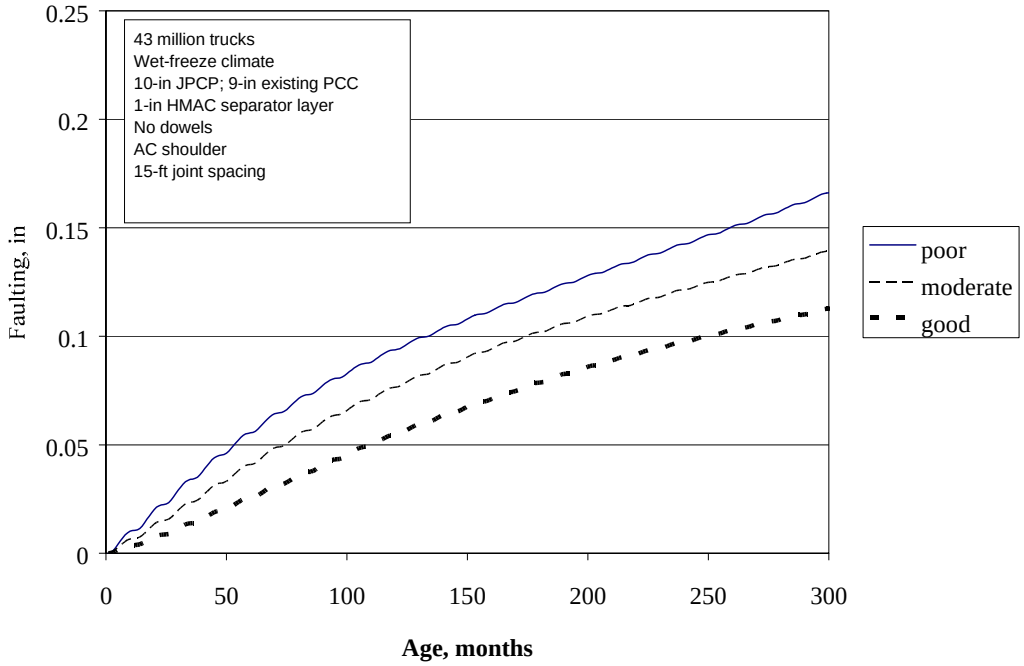

Figure 42. Plot showing the effect of existing PCC condition on predicted mean transverse joint faulting (for unbonded JPCP overlays).

Transverse Cracking

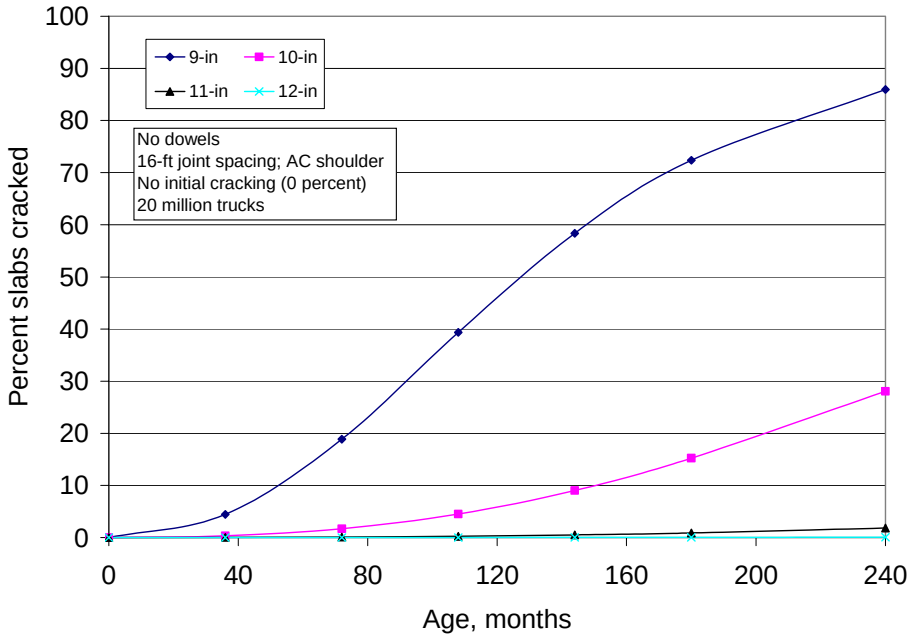

Figure 43. Plot showing the effect of slab thickness on overlay transverse cracking of unbonded JPCP overlays.

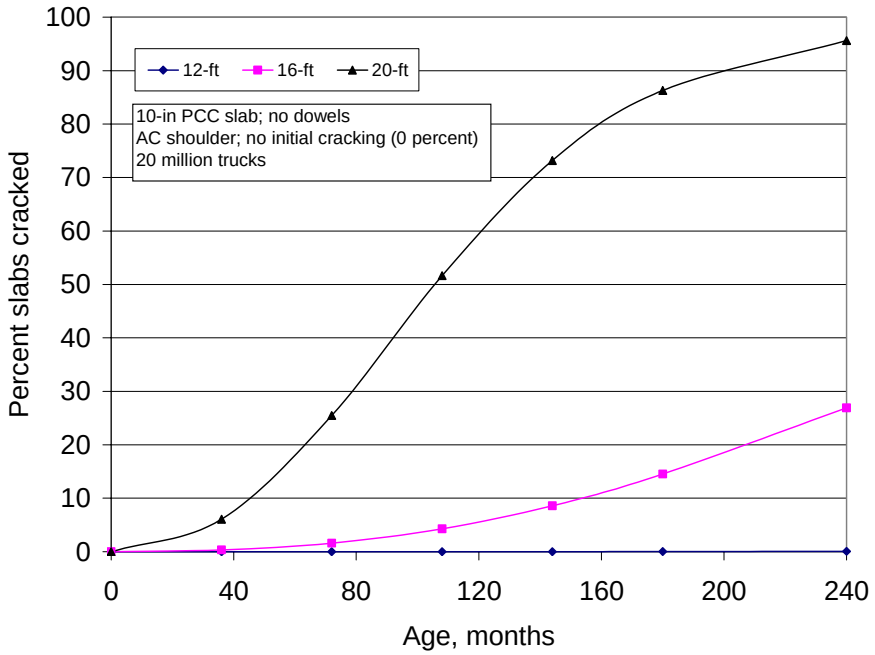

Figure 44. Plot showing the effect of joint spacing on overlay transverse cracking of unbonded JPCP overlays.

Bonded PCC over JPCP

Transverse Joint Faulting

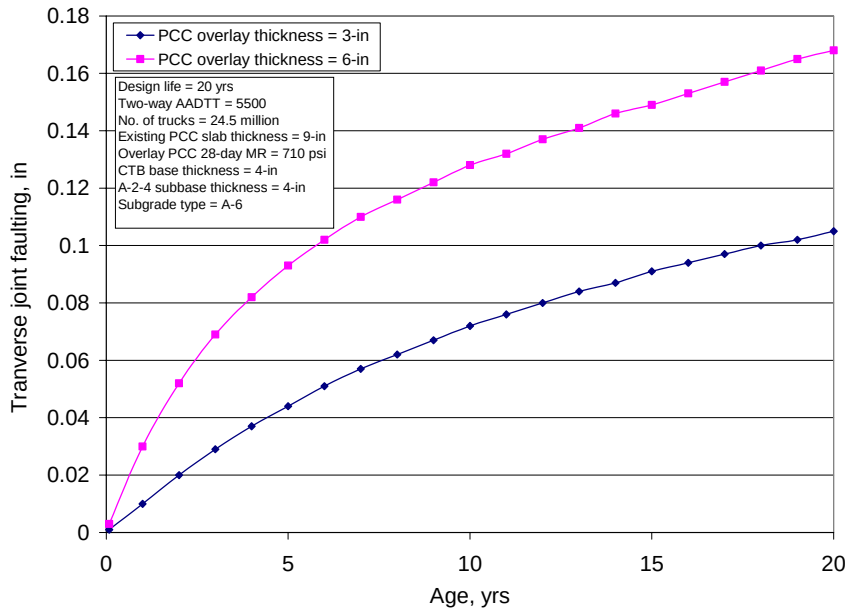

Figure 45. Plot showing the effect of PCC overlay thickness on transverse joint faulting of bonded PCC over JPCP overlays.

Transverse Cracking

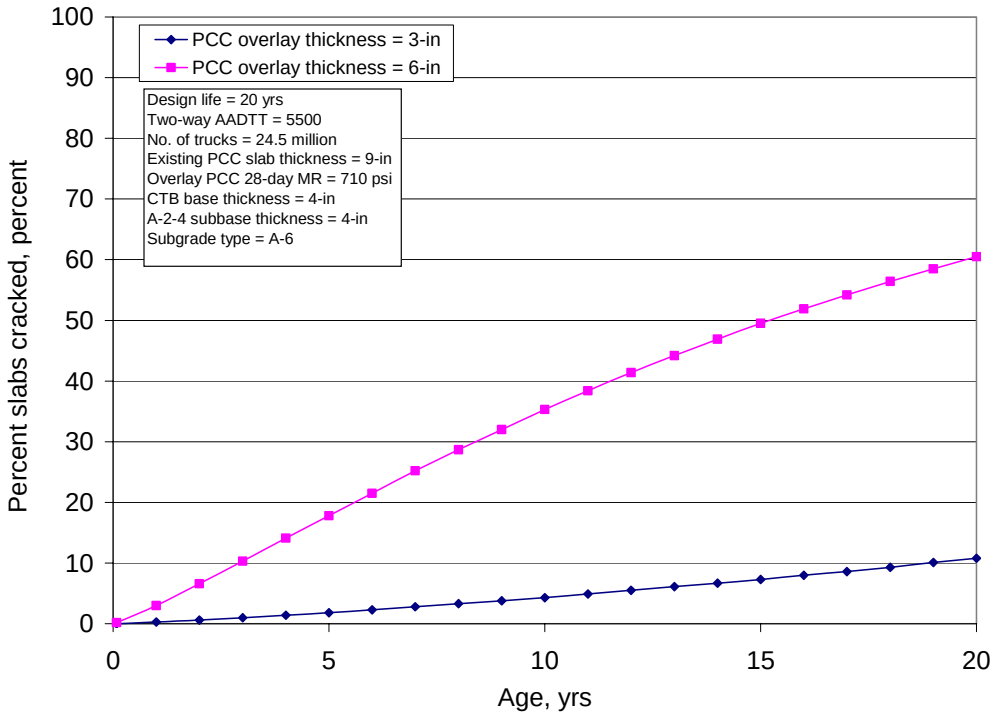

Figure 46. Plot showing the effect of PCC overlay thickness on transverse cracking of bonded PCC over JPCP overlays.

Unbonded CRCP over Existing PCC

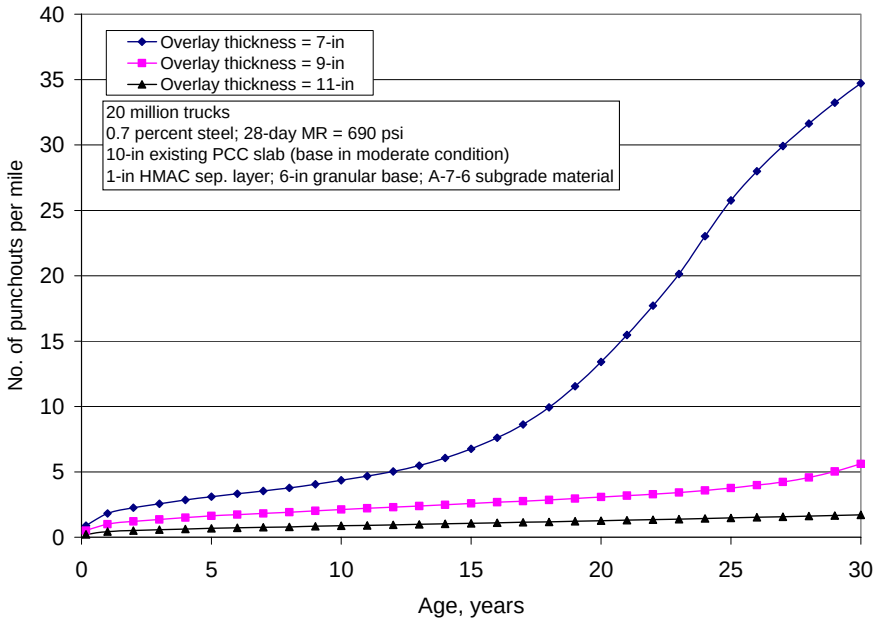

Figure 47. Plot showing the effect of overlay slab thickness on punchouts for unbonded CRCP overlays.

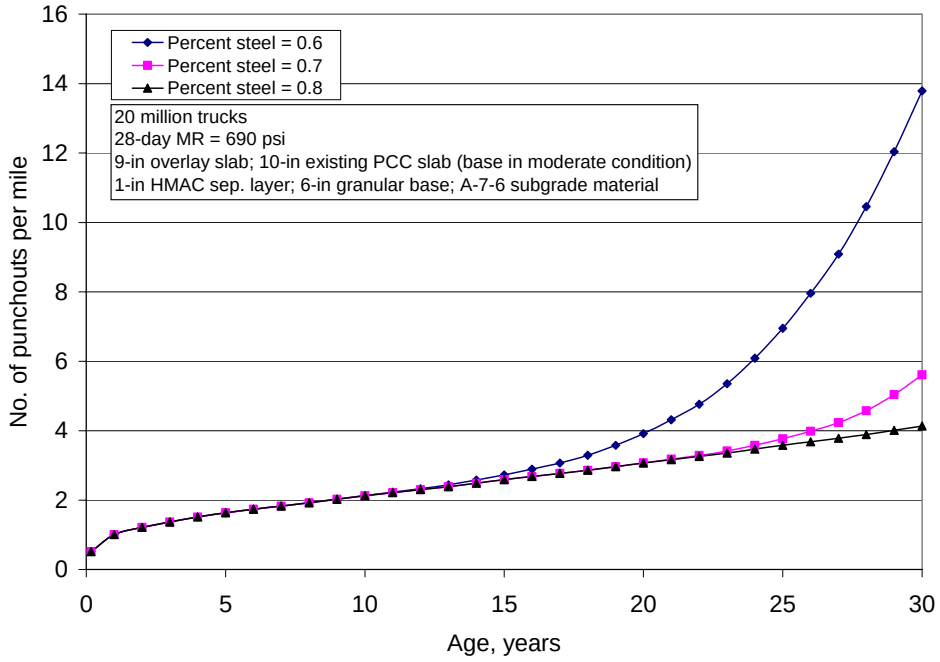

Figure 48. Plot showing the effect of the amount of longitudinal reinforcement on punchouts for unbonded CRCP overlays.

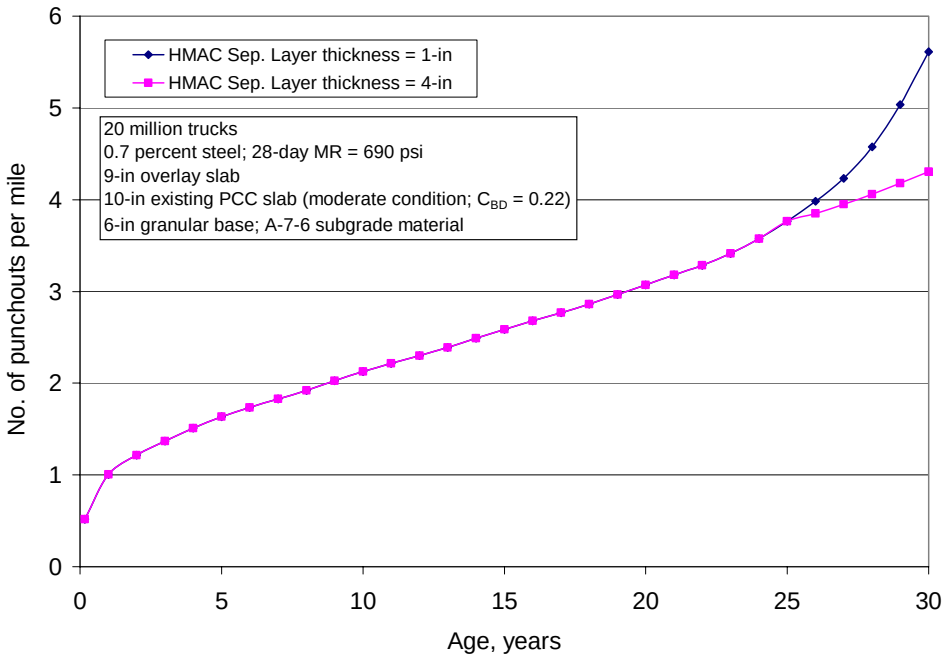

Figure 49. Plot showing the effect of HMAC separator layer thickness on punchouts for unbonded CRCP overlays.

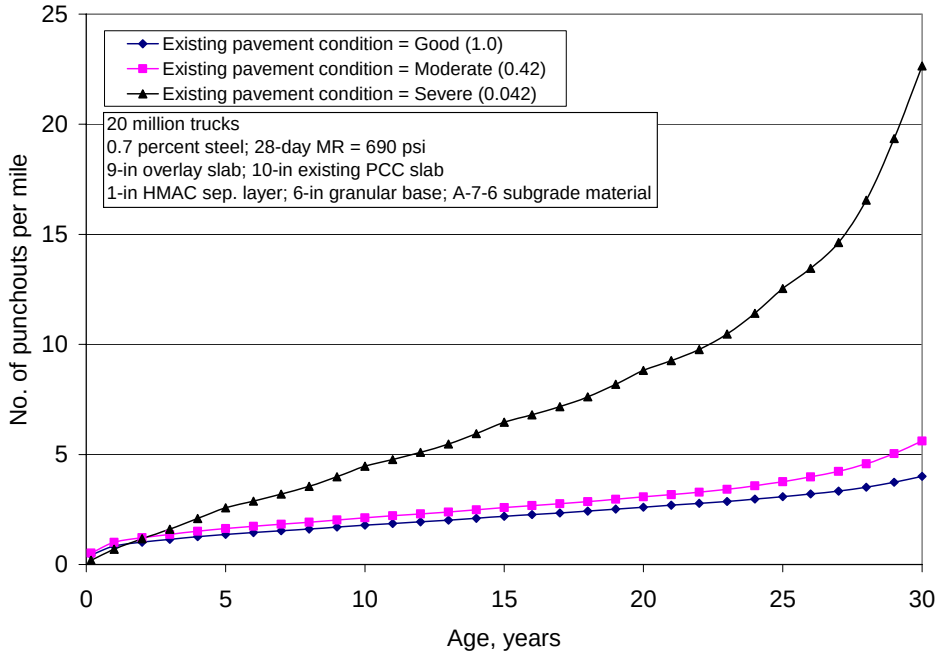

Figure 50. Plot showing the effect of existing pavement condition on unbonded CRCP overlays punchouts.

Bonded PCC over Existing CRCP

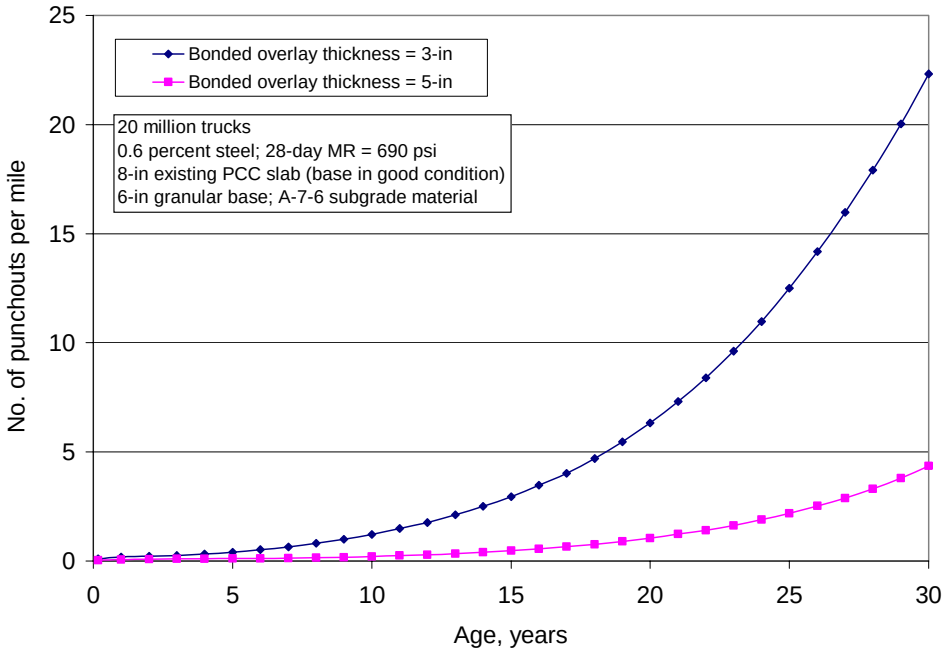

Figure 51. Plot showing the effect of overlay slab thickness on punchouts for bonded PCC over CRCP overlays.

JPCP Overlay over Existing Flexible Pavement

Transverse Joint Faulting

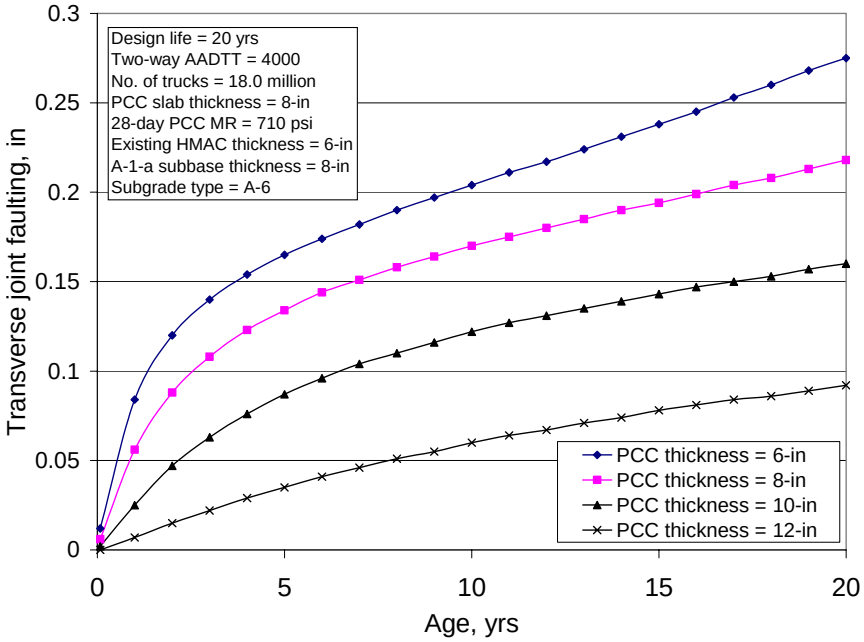

Figure 52. Plot showing the effect of overlay slab thickness on transverse joint faulting for JPCP overlay over existing flexible pavement.

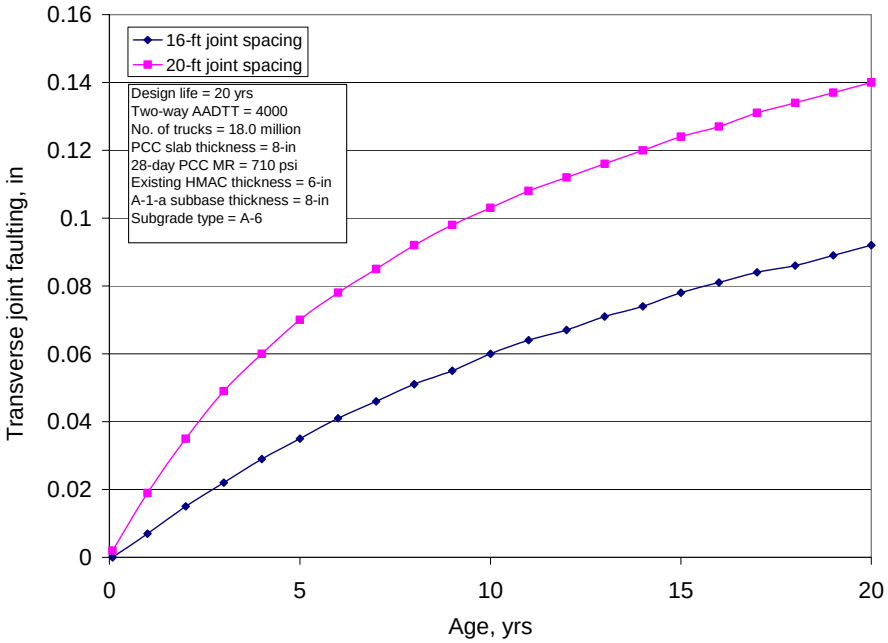

Figure 53. Plot showing the effect of JPCP overlay joint spacing on transverse joint faulting for JPCP overlay over existing flexible pavement.

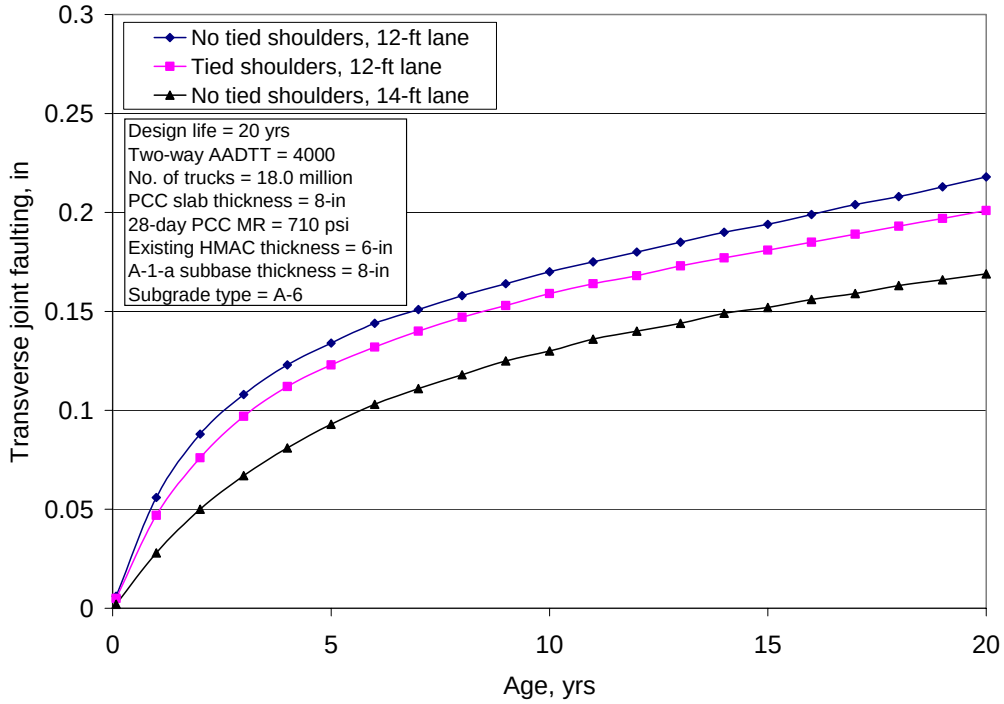

Figure 54. Plot showing the effect of JPCP overlay shoulder type (tied PCC or otherwise) and slab width on transverse joint faulting for JPCP overlay over existing flexible pavement.

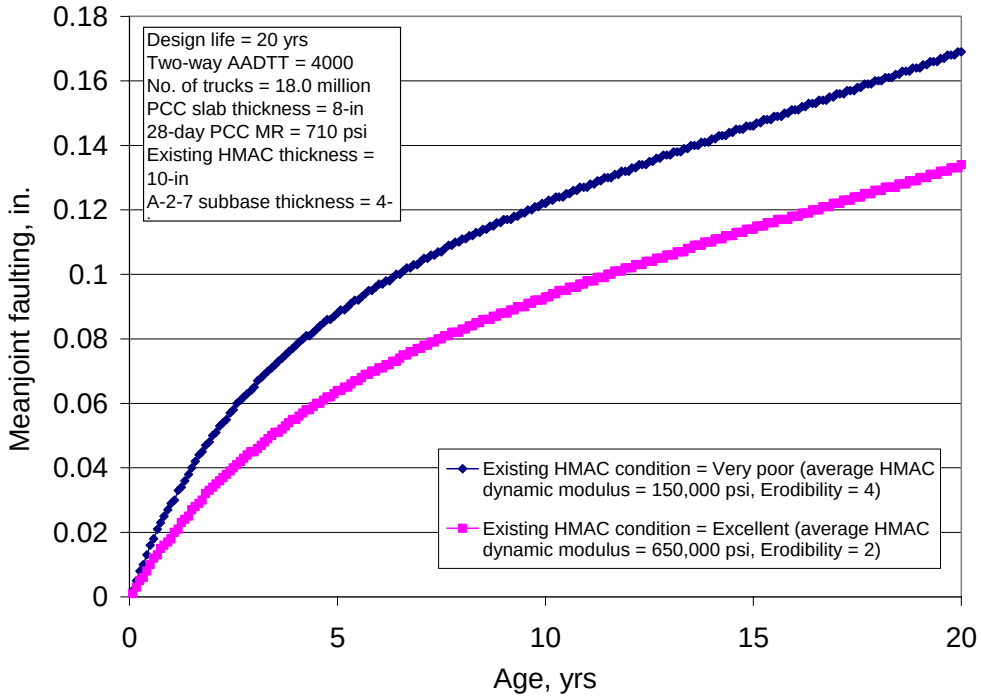

Figure 55. Plot showing the effect of existing HMAC condition on transverse joint faulting for JPCP overlay over existing flexible pavement.

Transverse Cracking

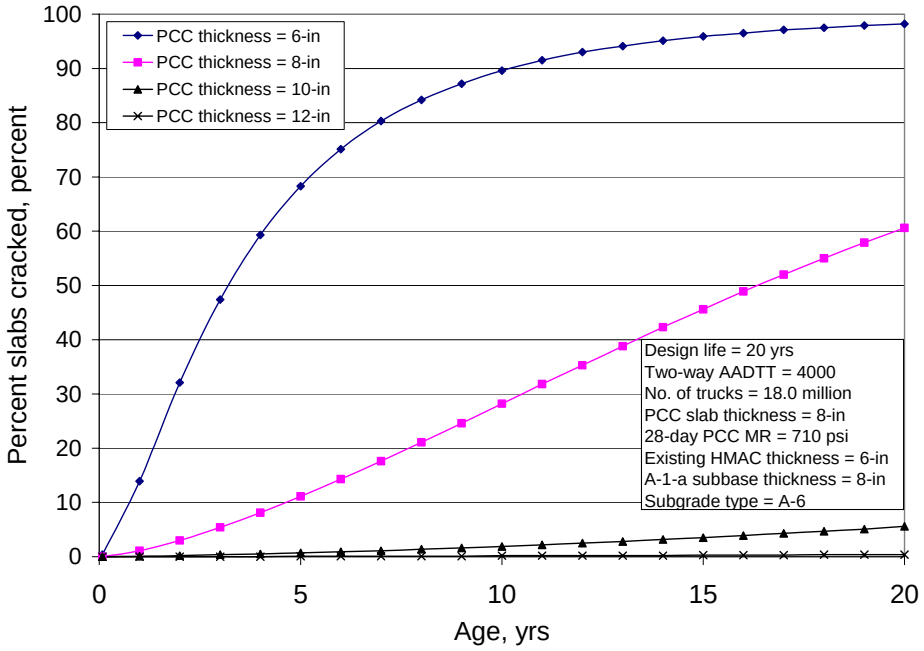

Figure 56. Plot showing the effect of overlay slab thickness on transverse cracking on transverse cracking for JPCP overlay over existing flexible pavement.

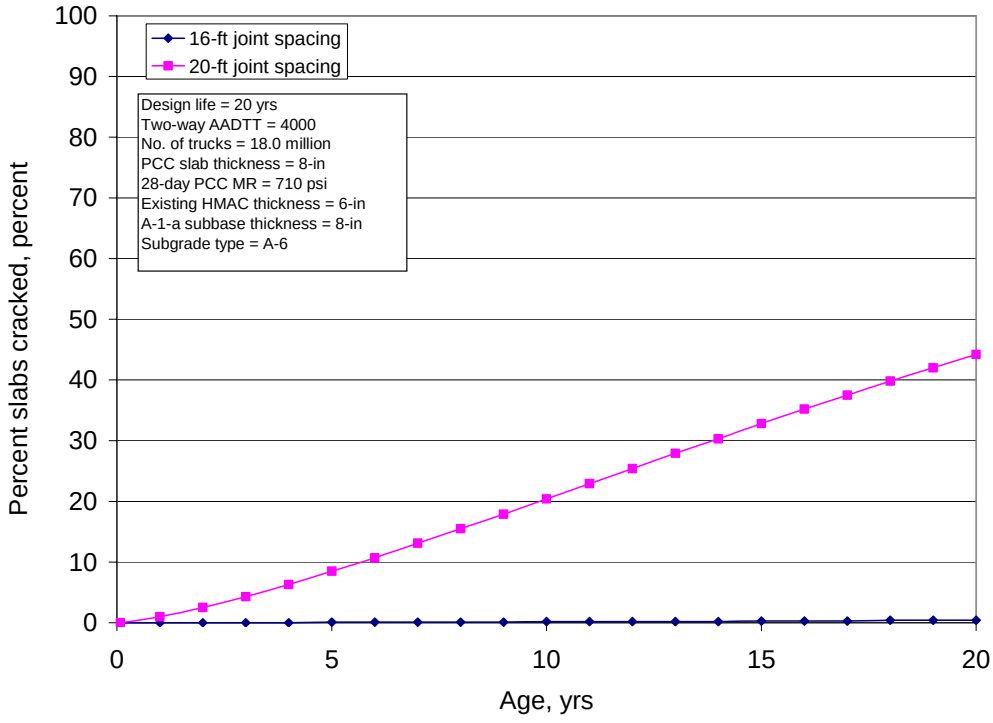

Figure 57. Plot showing the effect of JPCP overlay joint spacing on transverse cracking on transverse cracking for JPCP overlay over existing flexible pavement.

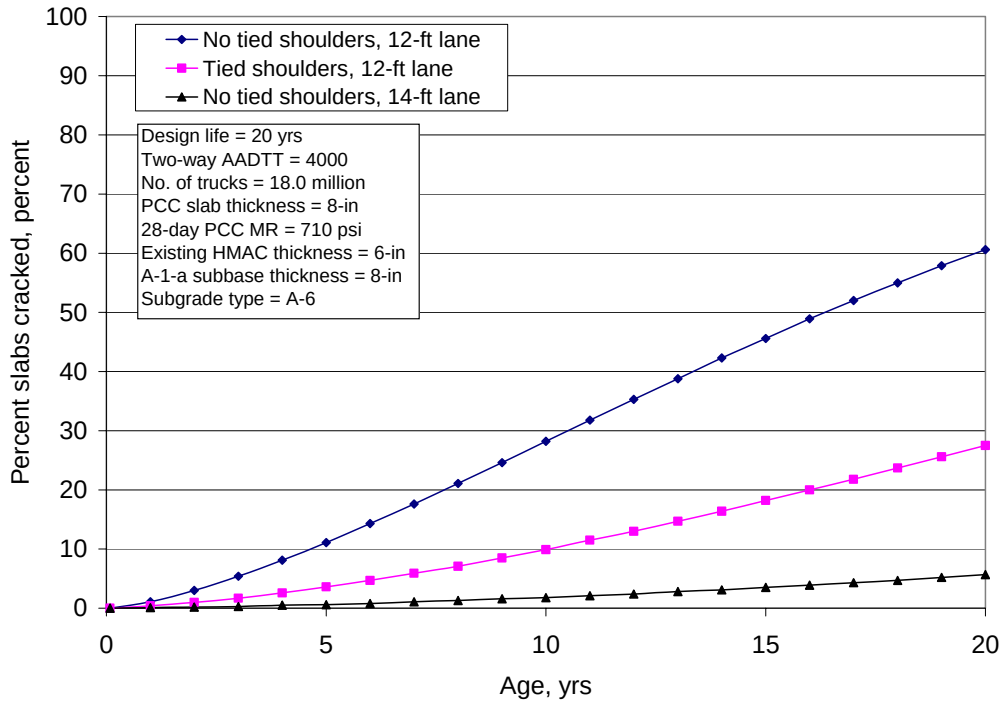

Figure 58. Plot showing the effect of JPCP overlay shoulder type (tied PCC or otherwise) and slab width on transverse cracking for JPCP overlay over existing flexible pavement..

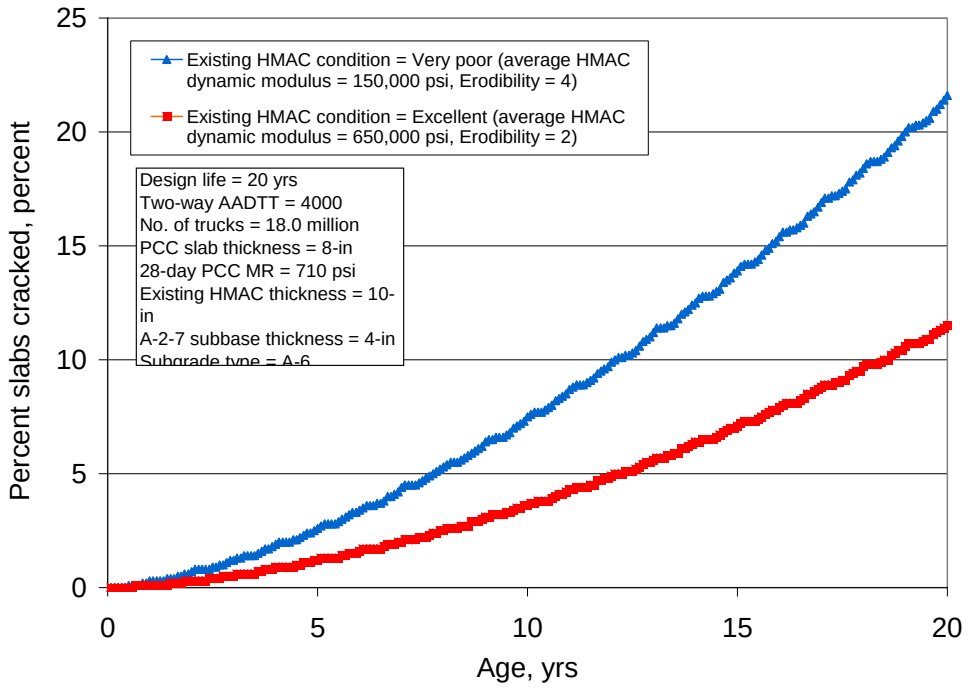

Figure 59. Plot showing the effect of existing HMAC condition on transverse cracking for JPCP overlay over existing flexible pavement.

CRCP Overlay over Existing Flexible Pavement

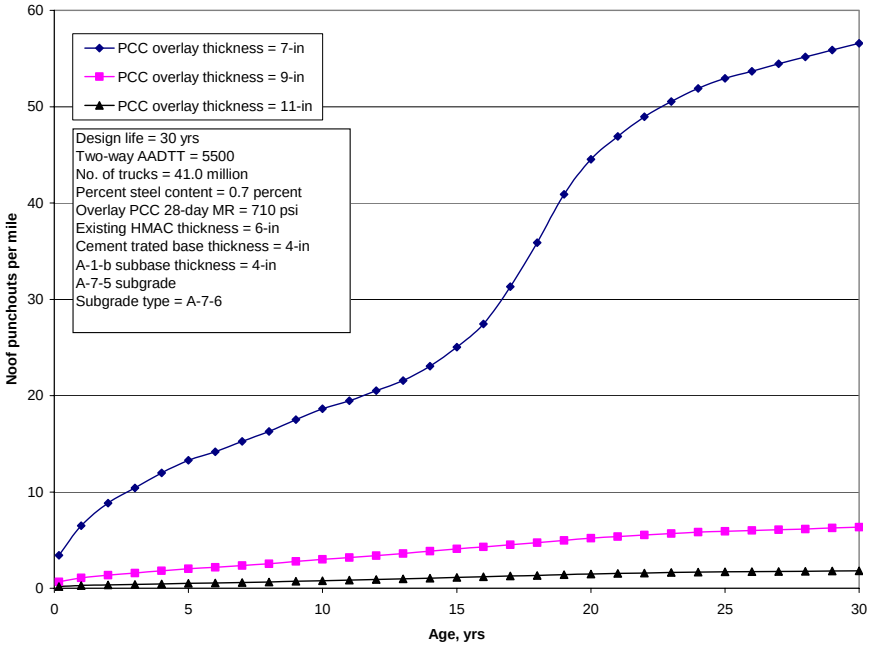

Figure 60. Plot showing the effect of overlay slab thickness on transverse cracking on punchouts for CRCP overlay over existing flexible pavement.

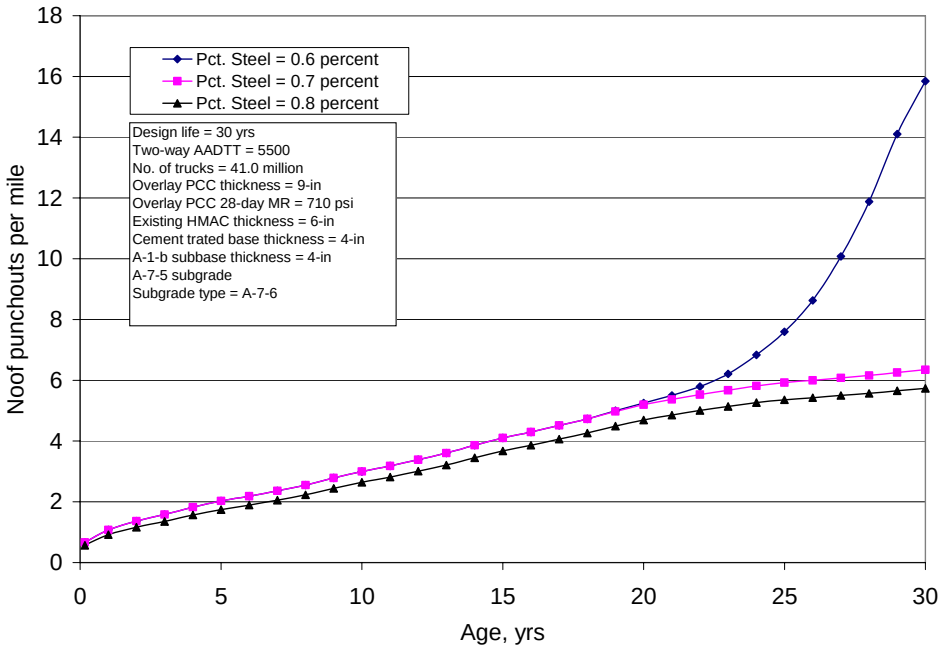

Figure 61. Plot showing the effect of overlay percent steel on transverse cracking on punchouts for CRCP overlay over existing flexible pavement.

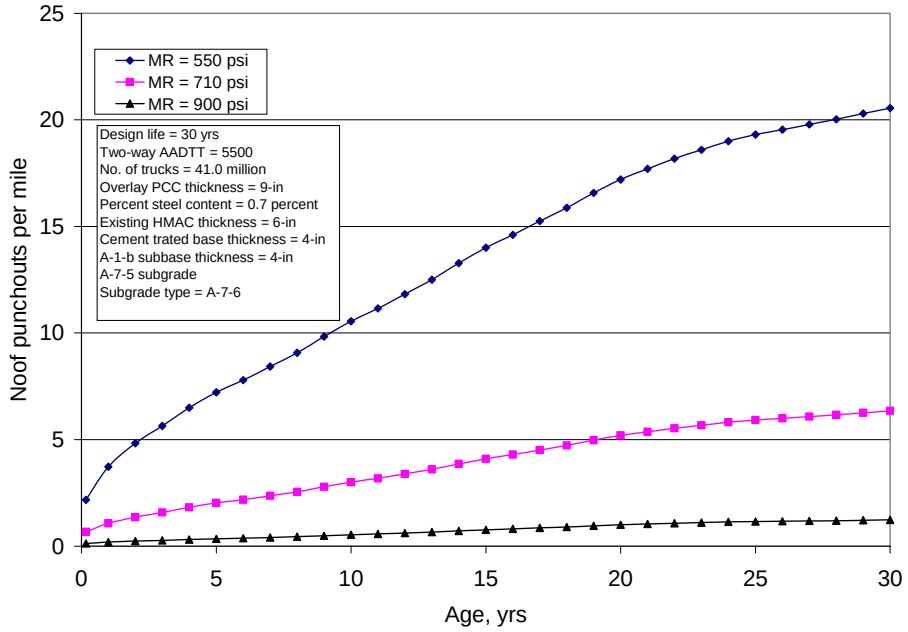

Figure 62. Plot showing the effect of overlay slab flexural strength on punchouts for CRCP overlay over existing flexible pavement.

Summary

The results of the sensitivity analyses were as expected. All of the effects tested affected the occurrence and progression of distress to a major extent. Key effects either as an increase or decrease in occurrence and progression of distress are summarized as follows:

- The use of dowels in overlays or for retrofitting existing JPCP as part of restoration significantly reduces predicted transverse joint faulting.
- Enhance slab edge support (use of widened slabs or tied PCC shoulders) also reduced predicted transverse joint faulting for restored JPCP and JPCP overlays.
- For bonded PCC overlays over existing JPCP or CRCP, increasing the overlay thickness significantly reduced distress (transverse joint faulting and transverse cracking for JPCP and punchouts for CRCP).
- The existing level of cracking after restoration significantly influence predicted future levels of transverse cracking.
- Reducing joint spacing for JPCP overlays reduced levels of predicted transverse joint faulting and transverse cracking for JPCP overlays.
- Increasing the PCC flexural strength and steel content generally reduced the levels of predicted punchouts for CRCP overlays.

In general, the models were sensitive to changes in puts and are suitable for modeling the occurrence and progression of distress for rehabilitation with PCC and hence PCC rehabilitation design.

REFERENCES

1. Carson, J.S., 2002. Model Verification and Validation, Proceedings of the 2002 Winter Simulation Conference, E. Yücesan, C.-H. Chen, J. L. Snowdon, and J. M. Charnes, eds.
2. Schlesinger, et al. 1979. Terminology for Model Credibility, Simulation, 32, 3,, pp. 103–104.
3. Rao, S., Yu, H. T., and M. I. Darter, The Longevity and Performance of Diamond-Ground Pavements, America Concrete Pavement Association, Skokie, IL, 1999.
4. FHWA, Datapave Version 3.0, Federal Highway Administration, Washington DC, 2001.
5. ERES Consultants, Inc., Evaluation of Unbonded Portland Cement Concrete Overlays, National Cooperative Highway Research Program, Washington DC, 1998.